



# Effective connectivity within the ventromedial prefrontal cortex-hippocampus-amygdala network during the elaboration of emotional autobiographical memories



Norberto Eiji Nawa<sup>a,b,\*</sup>, Hiroshi Ando<sup>a,b</sup>

<sup>a</sup> Center for Information and Neural Networks (CiNet), National Institute of Information and Communications Technology (NICT), Japan

<sup>b</sup> Graduate School of Frontiers Biosciences, Osaka University, Japan

## ARTICLE INFO

### Keywords:

Autobiographical memory  
Emotion  
Prefrontal cortex  
Hippocampus  
Dynamic causal modeling (DCM)

## ABSTRACT

Autobiographical memories (AMs) are often colored by emotions experienced during an event or those arising following further appraisals. However, how affective components of memories affect the brain-wide network recruited during the recollection of AMs remains largely unknown. Here, we examined effective connectivity during the elaboration of AMs - when retrieved episodic details are integrated to form a vivid construct - in the network composed by ventromedial prefrontal cortex (vmPFC), hippocampus and amygdala, three key regions associated with memory and affective processes. Functional MRI data was collected while volunteers recollected personal events of different types of valence and emotional intensity. Using dynamic causal modeling, we characterized the connections within the triadic network, and examined how they were modulated by the emotional intensity experienced during an event, and the valence of the affect evoked when recollecting the associated memory. Results primarily indicated the existence of a vmPFC to hippocampus effective connectivity during memory elaboration. Furthermore, the strength of the connectivity increased when participants relived memories of highly emotionally arousing events or that elicited stronger positive affect. These results indicate that the vmPFC drives hippocampal activity during memory elaboration, and plays a critical role in shaping affective responses that emanate from AMs.

## 1. Introduction

Emotions are integral to our memories. Past research has shown that memory encoding, consolidation and retrieval may be enhanced for events or stimuli experienced during moments of heightened arousal, i.e., high emotional intensity (Anderson et al., 2006; Denburg et al., 2003; Dolcos et al., 2005, 2004), and that the mechanisms enabling that are likely to be primarily mediated by the amygdala (Cahill et al., 1995, 1996; 1994; Hamann et al., 1999; LaBar and Cabeza, 2006), via its direct connections to the hippocampus (Fastenrath et al., 2014; Phelps, 2004). Though a vast body of animal and human research has examined how emotions influence the neural mechanisms underlying the acquisition and access of memories, much less attention has been paid to the interplay between emotions and memory processes during the recollection or elaboration of episodic autobiographical memories (AMs), when people contemplate or reminisce about past personal experiences. AM

elaboration is typically characterized by a subjective “sense of reliving”, sometimes referred to mental time travel, which often takes place when a memory is unfolded into a rich and vivid construct (Suddendorf et al., 2009). It may involve the reinstatement of emotional and mental states associated with but not necessarily identical to the original occurrence, as well as the re-experiencing of spatial, sensory and perceptual characteristics encountered during the event (Tulving, 1985; Wheeler et al., 1997).

The recollection of episodic memories, such as AMs, is widely thought to be a reconstructive process, in the sense that memories are conceived as being dynamic constructions made of different components that are integrated together to compose a whole representation of the original experience (Conway and Pleydell-Pearce, 2000; Schacter et al., 1998). Retrieval of AMs is commonly conceptualized as consisting of a *construction phase*, when a specific memory of the personal past is searched for and accessed (e.g., triggered by an external cue), which may be followed by an *elaboration*

\* Corresponding author. Center for Information and Neural Networks (CiNet), National Institute of Information and Communications Technology (NICT), Room 2A2, 1-4 Yamadaoka, Suita, Osaka, 565-0871, Japan.

E-mail address: [eiji.nawa@nict.go.jp](mailto:eiji.nawa@nict.go.jp) (N.E. Nawa).

<https://doi.org/10.1016/j.neuroimage.2019.01.042>

Received 23 July 2018; Received in revised form 8 January 2019; Accepted 17 January 2019

Available online 18 January 2019

1053-8119/© 2019 Elsevier Inc. All rights reserved.

phase, when episodic details related with that memory are further retrieved and integrated into a vivid construct, e.g., (Ford et al., 2014; McCormick et al., 2015). Though the distinction between these two phases can be more or less clear depending on how exactly AM retrieval is experimentally operationalized, previous studies have shown that the retrieval of personal memories as a whole recruits a large network of brain regions, most notably the hippocampus, the prefrontal cortex (including its ventromedial aspect), medial and lateral temporal structures (including parahippocampus), posterior midline regions, and lateral parietal cortex (Cabeza and St Jacques, 2007; Gilboa, 2004; Maguire, 2001; Svoboda et al., 2006). This network partially overlaps with the “default mode network” (Raichle, 2015; Raichle et al., 2001; Spreng and Grady, 2010), and is remarkably similar to the ensemble of areas engaged during episodic future thinking (Addis et al., 2007; Benoit and Schacter, 2015; Schacter et al., 2007, 2012), though not identical (Gilmore et al., 2018). Based on the observation that recollecting the past and imagining the future engaged a similar group of brain regions, it has been proposed that one possible overarching function of this brain-wide network could be to support various forms of “self-projection” (Buckner and Carroll, 2007), e.g., remembering the past, envisioning the future, conceiving the viewpoint of others, and possibly spatial navigation, though alternative views have been put forward to explain these commonalities as well (Hassabis and Maguire, 2009; Maguire and Mullally, 2013). The human hippocampus is the most well studied structure among the nodes in the putative AM retrieval network, and several theories have been proposed to explain the functions it possibly subserves (Bird and Burgess, 2008). Clarifying how the hippocampus interacts with other brain regions in each one of these capacities should provide a more specific characterization of the cognitive processes supported by this network, as well as the roles played by each one of its nodes.

Here, we focused on a portion of that large network, specifically, the network formed by the ventromedial prefrontal cortex (vmPFC), hippocampus and amygdala. These three regions have been consistently associated with autobiographical memory processes (Spreng et al., 2009; Svoboda et al., 2006), and hypothesized to play critical roles during the retrieval of emotional memories (Buchanan, 2007). The amygdala has been shown to be distinctively engaged in depressed individuals during the recall of emotional AMs compared to healthy controls, displaying enhanced activity during the recall of negative AMs, and decreased activity during the recall of positive AMs (Young et al., 2016); moreover, patients with damage to the hippocampus, amygdala and surrounding cortices have been shown to recall a lower proportion of negative AMs when compared to healthy controls and patients with damage only to the hippocampus (Buchanan et al., 2005), suggesting a critical role for the amygdala in the recall of emotional AMs. Though traditional views regarding the primary functions performed by the hippocampus and the amygdala have been challenged recently (Hassabis and Maguire, 2009; Janak and Tye, 2015; Maguire and Mullally, 2013; Rubin et al., 2017), the vast majority of studies focusing on these structures typically associate them with memory and emotion processes, e.g., (Phelps, 2004). In contrast, the area commonly referred to as the vmPFC is an intricate region both in terms of cortical and connectivity architecture (Glasser et al., 2016; Mackey and Petrides, 2014; Öngür et al., 2003; Öngür and Price, 2000) which has been associated with a multitude of functions spanning a wide array of different domains (Delgado et al., 2016; la Vega et al., 2016; Schneider and Koenigs, 2017). In studies involving autobiographical memories, the vmPFC has been mostly implicated with two distinct classes of processes, namely, processes related to the value or affective components associated with AMs, in line with the notion of a critical role played by the vmPFC in the generation of affective responses (Roy et al., 2012), and processes related to encoding, retrieval and consolidation of *schemas*, i.e., knowledge representations about regularities found in typical contexts or experiences that are abstracted from multiple episodes, and which influence the acquisition and retrieval of memories (Gilboa and Marlatte, 2017; van Kesteren et al., 2012). Related to the former, activity in the vmPFC has been shown to be modulated by subjective ratings of “likeness” and “dislikeness”, as well as “familiarity”,

regarding items appearing in specific AMs (Lin et al., 2016); moreover, the elaboration of positive AMs has been shown to induce greater activity in the vmPFC and other regions, when compared to neutral AMs (Speer et al., 2014). The vmPFC has also been shown to be engaged during the evaluation of the affective qualities of future scenarios (Benoit et al., 2014), and during the experience of positive emotions evoked by visual stimuli (Winecoff et al., 2013). In the realm of research investigating the processing of schemas, lesion studies seem to indicate that one specific deficit displayed by some vmPFC patients during memory retrieval is confabulation, which is most notably characterized by the retrieval of erroneous memories (Schneider and Koenigs, 2017). Though the exact mechanistic process that causes that impairment still needs to be clarified, taken together, these two lines of research suggest a double role for the vmPFC in the processes underlying the retrieval of AMs.

Although several studies have examined the functions possibly subserved by the vmPFC under a variety of contexts, much less is known about how the vmPFC, hippocampus and amygdala interact during autobiographical memory processes. In a study by McCormick et al. (2015), changes in functional and effective connectivity between the *construction* and *elaboration phases* involving the hippocampus and other regions were examined. During AM elaboration, it was found that the posterior hippocampus (bilaterally) exerted greater influence on visual areas, such as the middle occipital gyrus and the fusiform gyrus. No specific changes were observed with relation to vmPFC connectivity, and connectivity with the amygdala was not examined. Moreover, affective aspects of the AMs were not explicitly assessed in their analyses.

To further advance our understanding of the interactions that take place among the nodes in the putative AM retrieval network during the elaboration of personal memories, we used dynamic causal modeling (DCM) (Friston et al., 2003) to examine effective connectivity in the vmPFC-hippocampus-amygdala network. DCM enables the estimation of the directed influence a region exerts on other regions. Furthermore, it provides a principled way to compare candidate-models that differ with respect to those inter-region influences (reflecting different hypotheses regarding systems-level brain mechanisms underlying a given neuropsychological phenomenon (Stephan et al., 2010)). Modulatory effects in the connections within the triadic network caused by affective aspects of AMs, namely, emotional intensity experienced during an event, and the valence of the affect evoked when recollecting the associated memory were also assessed. We hypothesized that there would be a bidirectional interaction between vmPFC and hippocampus during memory elaboration, due to their involvement in schema processes and memory representation (Bonnici et al., 2012; Bonnici and Maguire, 2018; McCormick et al., 2017). Furthermore, we also expected to observe modulatory effects associated with emotional aspects of AMs in the connections within the triadic network, specifically in the connections departing from the regions thought to be involved in affective processes, vmPFC and amygdala, to the hippocampus.

## 2. Material & methods

### 2.1. Participants and study design

Thirty-six right-handed volunteers, all fluent Japanese speakers, initially took part in this study (22 females, mean age 22.3 years, range 20–25). Participants enrolled in the study by responding to an announcement sent to a mailing list of local university students interested in taking part in psychology/imaging experiments or via a part-time employment agency; most participants were undergraduate or graduate students at local universities. We limited the age range of the participants in order to minimize differences in the age of the recalled memories across participants. Other things being equal, female volunteers were given priority, since it has been shown that women recall more positive and negative life events than men (Seidlitz and Diener, 1998), and women recall more emotional information (previously acquired via a script) than men (Bloise and Johnson, 2007). All participants gave informed written

consent prior to participation in the laboratory sessions, in accordance with the principles stated in the Declaration of Helsinki. The study was approved by the local research ethics committee. All participants had normal or corrected-to-normal vision, and declared that they were not receiving treatment for psychiatric disorders at the time of the study.

The study was performed on 3 different days. On Day 0, prospective participants were directed to a web questionnaire, where they were asked to declare their age, gender, and evaluate a list of 110 verbal cues describing common life events, adapted from (Sharot et al., 2007; Speer et al., 2014) plus a few of our own. More specifically, participants were asked whether they could associate a personal memory with each one of the verbal cues, e.g., “Trip overseas”, and if that was the case, participants were asked to further evaluate their feelings when recalling that event using a single 7-point scale (1: Very negative, 4: Neither negative nor positive, 7: Very positive). Instructions emphasized that the memories did not have to exactly match the cues but could be only marginally related to them. Participants had the option of adding short descriptions of past personal events that were not covered by the initial 110 cues; those items were scored using the same scale. Based on the responses given by each participant on Day 0, cues were separated into three individual lists of negative (scores of 1 or 2), neutral (4), and positive events (6 or 7).

On Day 1, participants were invited to come to the laboratory to thoroughly evaluate the cues that were declared to be associated with a personal memory on Day 0. Several phenomenological aspects of each personal memory were assessed using questions from (Talarico et al., 2004) (see Section 2.2); for brevity, we excluded questions 2, 4, 17, 19, 21 and 22. Answers were given using a 7-point Likert scale; point labels differed slightly across questions but 1 always denoted ‘Low agreement’ and 7 always denoted ‘High agreement’. We also asked participants to rate the personal significance of the event, and the emotional intensity currently experienced when remembering that event (Addis et al., 2004), as well as the emotional intensity experienced during the original occurrence of the event. These questions were answered using a 5-point scale (point labels differed slightly across questions but 1 always denoted ‘Low’ and 5 always denoted ‘High’). Participants were also asked to report their age at the time of the event, and to estimate the number of times they had experienced similar events. We emphasized that if there were multiple occurrences of similar events, they should select one specific occurrence to perform the ratings. If any of the three lists generated on Day 0 (negative, neutral, positive) had fewer than 23 entries, participants were requested to add and evaluate additional events of the missing type until there were enough entries. Before evaluating the memories on Day 1, participants completed the Beck Depression Inventory (BDI-II) (Beck et al., 1996; Kojima et al., 2002), the Edinburgh Handedness Inventory (Oldfield, 1971) and the Positive and Negative Affective Scale (PANAS) (Watson et al., 1988). The PANAS was collected again at the end of Day 1. Finally, participants were invited to come back to the laboratory on Day 2 to take part in the imaging experiment (see Section 2.3). Similarly to Day 1, the general mood of the participants was assessed before and after the scanning sessions using the PANAS.

All 36 participants underwent the laboratory tasks on Days 1 and 2. However, 2 participants were unable to complete the imaging experiment, and 8 participants had a BDI-II score greater than 12 (a screening level adopted in other studies, e.g. (Leal et al., 2014)), resulting in a final cohort of  $N=26$  participants (14 females, mean age 22.3 years, range 20–25). For the participants in the final cohort, the time elapsed between Day 0 and Day 1 was on average 8.1 days ( $SD = 4.8$ , range from 1 to 18 days), whereas the time elapsed between Day 1 and Day 2 was on average 28.4 days ( $SD = 13.6$ , range from 1 to 46 days). Participants were monetarily compensated for their time on Days 1 and 2.

## 2.2. Autobiographical memories

On Day 1, participants rated among other phenomenological aspects the valence of the affect evoked when recalling an event, in both the positive and negative affective dimensions, by evaluating the statements

“While remembering the event, the emotions are extremely positive”, and “While remembering the event, the emotions are extremely negative”, respectively, using a 7-point Likert scale (1: Not at all, 7: Entirely) (questions 7 and 8, (Talarico et al., 2004)). Based on these responses, 3 revamped lists were compiled for each participant, (i) a list of “positive memories” (positive affect scores  $\geq 5$  and negative affect scores  $\leq 3$ ), (ii) a list of “negative memories” (positive affect scores  $\leq 3$  and negative affect scores  $\geq 5$ ), and (iii) a list of “neutral memories” (all the rest). “Positive memories” were sorted by the difference between positive affect scores and negative affect scores (descending order); “negative memories” were sorted by the difference between negative affect scores and positive affect scores (descending order), and memories in the “neutral” list were sorted by the sum of positive and negative affect scores (ascending order). If the “positive” or “negative” lists had fewer than 20 entries, we inspected the “neutral” list for cues that we judged could possibly elicit the target affect during memory elaboration, e.g., if trying to complete the list of “positive memories”, we looked for entries in the list of “neutral memories” that were added by the participant under the rubric “positive memory” but failed to meet the “positive memory” criterion, or alternatively, entries that had a positive dimension score  $\geq 5$  and a negative dimension score slightly above 3. If the “neutral” list had fewer than 20 entries, we inspected the “positive” and “negative” lists for entries that were originally classified under the rubric “neutral memory” but ended up in the “positive” or “negative” lists because of their scores, or alternatively, entries at the bottom of “positive” or “negative” lists that we judged were likely to elicit lower levels of positive or negative affect compared to the top entries of each list. After all these adjustments, we selected the top 20 entries of each list to be used as memory evoking cues in the imaging experiment of that particular participant. Note that this screening was performed only to maximize the chances of obtaining enough trials of each valence type: inside the scanner, participants were also requested to give ratings of evoked negative and positive affect after memory elaboration, together with ratings about the emotional intensity originally experienced at the event; those were the ratings that were ultimately used as inputs in the analyses (see Sections 2.6 and 2.7.1.1).

## 2.3. fMRI experimental paradigm

On Day 2, participants performed an AM retrieval task (Fig. 1) inside the scanner. At each trial, following a delay of 8–10 s (fixation), one of the 60 cues associated with a personal event was displayed on the screen (3 s), and participants were instructed to press the left button on a 4-button diamond-layout response pad as soon as they were able to start recalling that particular event. Participants were requested to recall the same events that were rated on Day 1. Following the button press, participants were told to continuously relive the original experience by

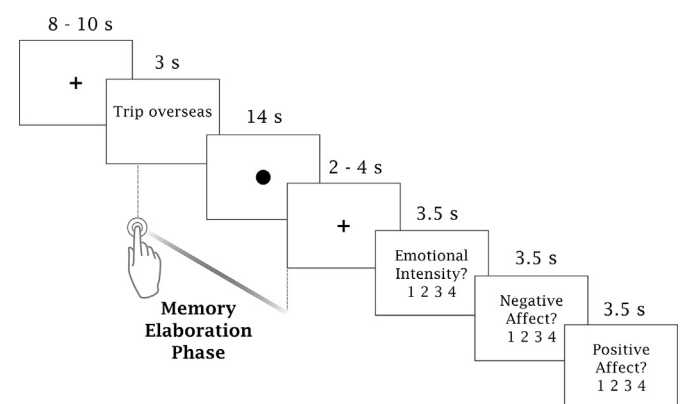


Fig. 1. One trial of the AM retrieval task. Participants were instructed to press a button as soon as they were able to recollect the event associated with the cue, and asked to continue to elaborate that particular memory until a fixation mark (+) appeared on the screen.

retrieving as many details as possible (memory elaboration phase). They were asked to keep recollecting the event while a small circle was displayed on the center of the screen (14 s). If for any reason the elaboration flow was interrupted before the end of that period, participants were instructed to press the right button of the response pad. After a short delay (2–4 s, fixation), questions were presented on the screen prompting participants to evaluate (a) the emotional intensity originally experienced in the event (4-point scale; 1: Not intense, 4: Very intense), (b) the negative affect experienced as they recalled the event (4-point scale; 1: Not negative at all, 4: Very negative), and (c) the positive affect experienced as they recalled the event (4-point scale; 1: Not positive at all, 4: Very positive), always in that order. Each question was displayed for 3.5 s, and participants were requested to give a response while the question appeared on the screen. We chose to ask participants to rate the emotional intensity experienced at the time of the event – as opposed to the emotional intensity experienced at recall time – because we judged that separating the temporal context of emotional intensity judgments and valence judgments would minimize the chances of confusing these two measures, making the task easier to perform. Using data collected on Day 1, we verified that the emotional intensity experienced during the original occurrence of the event was on average positively correlated with the emotional intensity experienced when remembering the event across participants (mean correlation coefficient  $r = 0.606$ , for all mean correlation coefficient calculations, the Fisher transform was applied to each participant's  $r$  before averaging, range between [0.182, 0.809], average number of datapoints per participant: 59.08). As expected, we also confirmed that the emotional intensity experienced during the event ( $M = 3.4$ ,  $SD = 0.5$ ) was on average judged to be greater than the emotional intensity experienced at recall time ( $M = 2.2$ ,  $SD = 0.5$ ; one-tailed paired  $t$ -test,  $t(25) = 19.048$ ,  $p = 1.064 \times 10^{-16}$ ). This strongly suggests that participants understood the difference between the two measures.

Twelve verbal cues were presented in each one of the 5 scanning sessions. Entries from the “positive”, “negative” and “neutral” lists were pseudo-randomly intermixed such that each session contained roughly the same number of cues from each class, and sequences of cues of the same type were not presented more than twice in a row. All participants in the final cohort completed the 5 sessions in the same day, without leaving the scanner. Participants were allowed to take breaks in between sessions, at their will. The AM retrieval task was implemented using the software Presentation v.18.2, (<http://www.neurobs.com>).

#### 2.4. Imaging data acquisition

A 3T Siemens Magnetom Trio whole-body MR scanner equipped with a standard 32-channel head-coil was used to acquire the imaging data. Participants entered the scanner after being briefed on MR safety and general procedures; they wore earplugs to attenuate scanner noise, a pneumatic belt to record respiratory cycles, and a transducer to monitor cardiac activity (index finger, left hand). Foam pads and towels were used to minimize head movement. First, 353 whole-brain functional images of resting-state data were acquired ( $T2^*$ -weighted multiband EPI (Moeller et al., 2008),  $TR = 1700$  ms;  $TE = 30$  ms; flip angle =  $70^\circ$ ;  $FOV = 192$  mm; voxel resolution =  $3.0$  mm iso; 50 axial slices; acceleration factor 2); participants were instructed to close their eyes but stay awake, and avoid repeatedly thinking about something in particular throughout the run. Resting-state data was collected before the AM retrieval task, in order to minimize the possibility that the performance of a cognitive task interfered with the resting-state data. Respiratory and cardiac data were only recorded during the resting-state session. (Resting-state data and physiological recordings are not presented.) That was followed by the acquisition of a whole-brain T1 MPRAGE anatomical image (1.0 mm iso) for coregistration and normalization purposes. That session lasted approximately 4 min, during which participants practiced the AM retrieval task. Though dummy cues were used during training, participants were asked to familiarize themselves with the task by performing all steps as instructed before entering the scanner. Next, one T2

TSE image was acquired for automatic probabilistic parcellation of the hippocampal subfields (Yushkevich et al., 2014), covering the area of interest bilaterally (30 slices perpendicular to the long axis of the hippocampus; in plane resolution =  $0.4 \times 0.4$  mm, slice thickness =  $2.0$  mm; data not used in the current analysis). Finally, participants underwent 5 sessions of the AM retrieval task. In each session, 288 whole-brain functional images were acquired using the same scanning parameters as in the resting-state session. Participants held a response box (4-button, diamond layout, by Current Designs, <http://www.curdes.com>) in their right hands to record behavioral responses, and a squeeze ball for emergency purposes in their left hands. Sessions where excessive head movement was detected (displacements  $> 3$  mm or rotations  $> 2^\circ$ ) were excluded from the analyses (2 participants, one session each).

#### 2.5. Imaging data processing and analysis

Effective connectivity analysis using DCM on the vmPFC-hippocampus-amygdala network was performed on native-space data; however, to determine peaks of activity on an individual participant basis, we first performed a group-level analysis based on data normalized to the Montreal Neurological Institute (MNI) template space, and located group-level peak voxels in the vmPFC, hippocampus and amygdala. Details of the procedure are described below.

##### 2.5.1. Preprocessing pipeline

Imaging data were processed and analyzed using Statistical Parameter Mapping (SPM12, v6685, Wellcome Trust Center for Neuroimaging, London, UK, RRID:SCR\_00703) and custom-made code implemented in Matlab (version R2016a, RRID:SCR\_001622). The first 3 images of each functional session were discarded to allow for magnetic field stabilization. The functional images collected during the AM retrieval task were first spatially realigned within and across sessions using a rigid body transformation to correct for head movement (the first image of each session, and the first image of the first session used as references), and unwrapped in order to correct for gradient-field inhomogeneities caused by motion. The T1 anatomical image of each participant was coregistered to the mean functional image generated after realignment/unwarping. During the same process, the native-space masks of the regions-of-interest (ROIs) were also coregistered to the mean functional image (see Section 2.5.2 for the generation of native-space masks). Functional images used to locate group-level peak voxels were normalized to the MNI template space by applying parameters derived from the normalization of the participant's T1 anatomical image to the MNI/ICBM template (East Asian brains). The normalized images were rewritten at 2 mm isometric voxels, and spatially smoothed with a 6 mm full-width half-maximum Gaussian kernel (FWHM). Functional images used in the DCM analysis were not normalized. Moreover, to prevent the mixing of signal from adjacent areas, spatial smoothing was performed for each one of the ROIs individually using the masks generated in the parcellation of individual T1 anatomical images, following a procedure similar to the one employed in (Fastenrath et al., 2014). We were particularly concerned with the anterior hippocampus and the amygdala since they sit close together in the medial temporal region. ROI-specific smoothed images were generated by using the masks for the hippocampus, amygdala, vmPFC (*medial-orbitofrontal + rostral anterior cingulate*), plus a mask of the rest of the brain (excluding the 3 ROIs) to generate region-specific images containing only one of the regions but not the others. Each one of those images was smoothed independently (FWHM = 6 mm), and the resulting images were then recombined to form a single smoothed functional image of the entire brain.

##### 2.5.2. Automatic parcellation of T1 anatomical image

Voxel timeseries employed in the DCM analysis were collected from imaging data in native-space, i.e., non-normalized data. To determine the location of voxel clusters within the hippocampus, amygdala and vmPFC of each participant, anatomical masks of these ROIs were generated based on the results of the automatic parcellation of individual T1 anatomical images

performed using Freesurfer (version 5.3.0, RRID:SCR\_001847), using the script *recon-all*. Labeling of cortical areas was based on the Desikan-Killiany atlas (Desikan et al., 2006), whereas labeling of subcortical structures was done using the probabilistic atlas included with the Freesurfer distribution (Fischl et al., 2002). The vmPFC is not a discrete structure with clear-cut anatomical boundaries (Zald and Andreotti, 2010); therefore, for the purposes of localizing the vmPFC in native-space, we used a mask which was the union of the *medial-orbitofrontal* and the *rostral anterior cingulate*, as determined by the automatic parcellation of each participant's anatomical image. All masks were coregistered to the mean functional image of the AM retrieval task sessions, together with the participant's T1 anatomical image, in the coregistration step described above.

## 2.6. Behavioral data

We assessed the consistency of the subjective ratings of emotional intensity experienced during the original event, and the evoked positive and negative affect during memory elaboration by computing the Pearson correlation coefficient ( $r$ ) between the values reported on Day 1 (days before scanning) and Day 2 (inside the scanner), after converting the ratings to z-scores (standard score) within each measure, participant, and day. We also examined correlations between the 3 ratings given inside the scanner. In order to examine whether there were differences in memory access time, i.e., the time elapsed between the onset of the verbal cue until the button press acknowledging successful memory construction, associated with emotional intensity or valence, we separated the reaction times (RTs) into different types based on the ratings given inside the scanner on Day 2. Trials were divided into 2 emotional intensity types (Low Emotional Intensity: trials where emotional intensity ratings were 1 or 2; High Emotional Intensity: trials where emotional intensity ratings were 3 or 4; data from trials with missing emotional intensity ratings were not included) or 3 valence types (Negative: trials where negative affect ratings were 3 or 4, and positive affect ratings were 1 or 2; Neutral: trials where negative and positive affect ratings were 1 or 2; Positive: trials where negative affect ratings were 1 or 2, and positive affect ratings were 3 or 4; data from trials where both affect ratings were high (3, 4) or with missing affect ratings were not included). We then computed the average RT of each trial type for each one of the participants, and entered the data in a two-sided paired-samples  $t$ -test (emotional intensity) or in a one-way repeated measures analysis of variance test (rmANOVA) (valence). For the rmANOVA, Greenhouse-Geisser correction was used to adjust degrees of freedom and  $p$ -values, whenever the Mauchly's sphericity test was significant, and exploratory post-hoc tests were corrected for multiple comparisons using Bonferroni correction. Using the same trial type classification, we also examined whether there were differences in average emotional intensity ratings given inside the scanner across trials of different valence types (Negative/Neutral/Positive), and likewise, whether there were differences in average evoked positive or negative affect across trials of different emotional intensity types (Low/High Emotional Intensity). In addition, we also checked for differences in memory age, i.e., the number of years that had elapsed since the occurrence of the event until the time of the test (participant's age on scanning day – age at the time of the event, in years), and personal significance of the event across different trial types, based on the ratings obtained on Day 1. All tests were performed using Matlab or SPSS (version 24, RRID:SCR\_002865).

## 2.7. Examining effective connectivity in the vmPFC-hippocampus-amygdala network during memory elaboration using DCM

### 2.7.1. Identifying group-level peak voxels (MNI normalized) to guide the extraction of timeseries data (native-space)

**2.7.1.1. General linear model (MNI normalized).** Because DCM analysis can only yield meaningful results when it is based on timeseries data from

areas that respond to the experimental manipulation (Stephan et al., 2010), precisely locating such voxels in each one of the participants is critical. That can be done in a standard stereotaxic space, such as the MNI, or in each participant's native-space. We chose to extract the timeseries used in the DCM analysis from native space data to minimize ambiguities when locating clusters in subcortical structures. As a first step, two general linear models (GLM) were computed based on normalized data to locate appropriate peak voxels in the vmPFC, hippocampus and amygdala at the group-level. In order to examine effects associated with emotional intensity experienced during the original event, group-level peak voxels were determined by computing a GLM where the brain activity recorded during the memory elaboration phase, i.e., when details about the event are recalled to form a vivid construct, was modeled as boxcar function that started with the button press indicating that a memory had been found, and ended at the start of the fixation period preceding the screens that prompted for evaluations of emotional intensity, evoked negative and positive affective. In the DCM framework, modulatory effects are examined by separating trials into different types according to the experimental manipulation. Therefore, trials were classified using the same criteria described in Section 2.6; to assess effective connectivity effects associated with emotional intensity, the memory elaboration phase was divided into two regressors, one containing the High Emotional Intensity trials, and another containing the Low Emotional Intensity trials. Note that memories of different valence became intermixed in both High and Low Emotional Intensity regressors. Trials with missing emotional intensity ratings were modeled using a separate regressor. In a similar way, to assess effective connectivity effects associated with evoked valence, an identical GLM was computed but this time the memory elaboration phase was split into three regressors, Positive, Negative, and Neutral. Trials where both affect ratings were high (3 or 4) or with missing affect ratings were modeled using separate regressors. In both GLMs, the memory elaboration phase was only modeled for the trials where participants indicated successful memory construction by pressing the left button following the verbal cue. In trials where memory elaboration was interrupted, the length of the boxcar function was adjusted to match the second button press. Verbal cues and rating screens were modeled as event-related responses (delta functions) positioned at the onset of each event. Fixation screens and button presses were not entered in the model. Delta functions and boxcar functions were then convolved with the canonical hemodynamic response function implemented in SPM to generate the predicted blood-oxygenation level dependent (BOLD) responses. The six movement parameters derived from the realignment step (3 to account for rigid-body translations, and 3 to account for rigid-body rotations) served as regressors of no interest, and an autoregressive AR(1) model was used to correct for timeseries correlations in the data during model parameter estimation. A highpass filter (cutoff 128 s) was applied to remove slow signal drifts.

The contrasts [*High Emotional Intensity* – *Low Emotional Intensity*], [*Negative* – *Neutral*], and [*Positive* – *Neutral*] were calculated based on the resulting parameter estimates, and used to verify the effectiveness of the manipulations. Finally, the contrasts [*High Emotional Intensity* + *Low Emotional Intensity*] and [*Positive* + *Neutral*] were used to determine the group-level peak voxels that would serve to guide the search for peak voxels in native-space data. The condition *Negative* was excluded when determining the peak voxels for the evoked valence DCM for reasons that will be clarified below (Results).

We restricted the DCM analysis to regions in the left hemisphere; even though evidence of clear lateralization is still mixed, especially with regard to the hippocampus (Piefke et al., 2003; Ryan et al., 2001; Viard et al., 2007), AM retrieval processes have been reported predominantly on left-lateralized regions (Addis et al., 2004; Cabeza and St Jacques, 2007; Conway et al., 1999; Gardini et al., 2006; Gilboa, 2004; Maguire, 2001; Maguire and Frith, 2003; Maguire and Mummery, 1999; Piolino et al., 2009; Svoboda et al., 2006). The group-level peak voxels were used as reference points to locate individual clusters of activation in each

participant's native-space data (see Section 2.7.2.3). This two-step approach was adopted to improve the chances that the native-space clusters (from where the timeseries employed in the DCM analysis were ultimately extracted) were compatible across participants, and to better account for individual differences in anatomy and function that may exist across participants (Fastenrath et al., 2014). Inaccurately or inconsistently determining signal sources can be especially harmful to network modeling analysis (Smith et al., 2011). This is particularly relevant when dealing with relatively large structures that are likely to show some degree of spatial specialization, such as the anterior/posterior distinction within the hippocampus (Poppenk et al., 2013; Zeidman and Maguire, 2016), and/or have been associated with a variety of different functions and domains, such as the vmPFC (Delgado et al., 2016; la Vega et al., 2016).

**2.7.1.2. Group-level analysis (ROI analysis, MNI normalized).** First-level contrasts obtained in the previous step were entered into a group-level analysis, with participant as random factor. One-sample t-tests were performed using small-volume correction on the voxels in the vmPFC, hippocampus and amygdala. Masks for the ROIs were defined using the Harvard-Oxford anatomical atlas, as implemented in FSL. For the purposes of determining the group-level peak voxel in the vmPFC, we used the mask *Frontal Medial Cortex*, but only considered clusters of activation with centers located in or below the plane defined by  $Z = 0$  in the MNI stereotaxic space (Delgado et al., 2016). Peak voxels were determined for each one of the regions (small-volume correction), using family-wise-error correction for multiple comparisons (FWE) implemented in SPM, at a height threshold of  $p < 0.05$ .

## 2.7.2. Extracting individual ROI timeseries data (native-space)

**2.7.2.1. Converting group-level peak voxel coordinates (MNI) to native-space coordinates.** The group-level peak coordinates determined in the previous step were individually converted to native-space coordinates to serve as reference points when searching for peaks of activity in the vmPFC, hippocampus and amygdala. For each participant, conversion was done by employing the following procedure: (1) single voxel masks located at the MNI group-level peak voxels in the vmPFC, hippocampus and amygdala, plus spherical masks centered at the same voxels (arbitrary radius of 5 mm) were generated to help visually locate the peak voxels in native-space; (2) to project the masks in MNI space to native-space, parameters of the inverse affine transform (MNI  $\rightarrow$  native-space) for the target participant were obtained as a by-product of the SPM Segment utility used to segment the participant's T1 anatomical image into gray matter, white matter and cerebrospinal fluid; (3) all MNI masks were converted to the participant's native-space by applying the inverse affine transform using the SPM Deformations utility; (4) the coordinates of the converted group-level peak voxels in each participant's native space were determined by visually inspecting the resulting masks using *fsleyes* (FSL).

**2.7.2.2. Creating masks to locate the native-space peak voxels.** The converted group-level peak voxels may not necessarily map into voxels that show significant effects in the individual dataset of each one of the participants. Therefore, we had to examine the voxels in the vicinity of the group-level peak voxels to determine whether there were native-space peak voxels that would satisfy the following conditions: (1) they should be located within a certain radius (8 mm) around the group-level peak voxels, so to maximize consistency across participants, and (2) they should be located within the anatomical boundaries of individual hippocampus, amygdala, and vmPFC (the union of the *medial-orbitofrontal* and *rostral anterior cingulate*). Additional masks were created to accomplish that; first, 8-mm spheres centered on the converted group-level peak coordinates were generated using the SPM toolbox Marsbar (RRID:SCR\_009605) to roughly delimit the search space boundaries,

similarly to other studies, e.g., (Fastenrath et al., 2014; Seghier et al., 2010). Next, a mask was created from the intersection of each one of the 8-mm spheres with the anatomical mask of the corresponding ROI to guarantee that if native-space peak voxels were identified, they would necessarily satisfy the 2 conditions above.

**2.7.2.3. Locating individual native-space peak voxels.** Individual GLMs based on the ROI-specific smoothed, native-space data of each participant were computed using the same specifications used to build the models employed to locate group-level peak voxels. The resulting parameter estimates were used to calculate the contrasts [*High Emotional Intensity + Low Emotional Intensity*] and [*Positive + Neutral*], and the masks created in the previous step were used to identify individual peak voxels in the hippocampus, amygdala and vmPFC. No statistical threshold was specified at this stage. If appropriate voxels were located, 10-mm spheres centered on them were generated using Marsbar. Finally, the intersection between the 10-mm spheres with the anatomical mask of the corresponding region was computed to determine the voxels from which the timeseries employed in the DCM analysis were extracted.

**2.7.2.4. Extracting individual timeseries data.** The SPM Volume of Interest utility was employed to extract timeseries data from the voxels determined in the previous step. A threshold of  $p < 0.05$  (uncorrected) was employed to determine the source voxels in the region delimited by each mask, in line with other studies, e.g., (Fastenrath et al., 2014). Valid timeseries can only be extracted if there are supra-threshold voxels within the boundaries of the target region. Timeseries were extracted from unsmoothed, native-space data as the first eigenvariate across supra-threshold voxels, and were adjusted for 'effects of interest', i.e., they were mean-corrected and rectified based on the movement parameters obtained after spatial realignment.

## 2.7.3. DCM analyses

Dynamic Causal Modeling (DCM) (Friston et al., 2003) is a method for estimating effective connectivity across brain regions, or *nodes*, i.e., how neural activity in one brain region affects activity in another (Friston, 2009). In a typical situation, there will be different candidate-models (hypotheses) regarding the characteristics of the underlying network subserving a given cognitive function, e.g., how nodes are interconnected via directed links to each other, or which connections are affected by external modulatory effects. DCM can determine the model that most parsimoniously explains the observed data among the assessed models, if there is one, providing a principled way to compare different hypotheses regarding the directions and connectivity strengths of the network connections, and thus, enabling inferences about directed couplings between brain regions (Stephan et al., 2010). Under the same framework, DCM also allows one to examine how external modulatory effects influence the strength of connections, i.e., whether and how experimentally controlled manipulations affect the effective connectivity exerted by one node onto another. Here, the DCM analysis was performed using functions provided with SPM 12 (release 6685, DCM12). Our models consisted of 3 nodes, i.e., the vmPFC, left hippocampus, and left amygdala. Nodes in the models were fully interconnected via intrinsic forward and backward connections, resulting in 6 connections in total (Fig. 2). A large body of human and animal studies indicates the existence of reciprocal connections linking these regions, via direct and indirect (polysynaptic) pathways (Eichenbaum, 2017; Kim and Whalen, 2009; Öngür and Price, 2000; Preston and Eichenbaum, 2013; Saunders et al., 1988; Simons and Spiers, 2003). Moreover, meta-analytic studies based on human neuroimaging studies show that these regions often coactivate (la Vega et al., 2016; Spreng et al., 2009), likely reflecting the underlying systems-level organization of this set of regions.

In the DCM framework, experimental manipulations enter the model as external inputs. Such inputs may directly drive the nodes in the model (driving inputs) or modulate the effective connectivity of its connections

(modulatory inputs). For the High/Low Emotional Intensity analysis the driving input was generated by concatenating the onsets (with the respective durations) of the memory elaboration periods from all trials with a valid emotional intensity rating (in effect, the union of the High Emotional Intensity and the Low Emotional Intensity regressors). Likewise, for the Positive/Neutral analysis the driving input was generated by concatenating the onsets (with the respective durations) of the memory elaboration periods from all trials with valid Negative and Positive affect ratings (in effect, the union of the Negative, Neutral and Positive regressors). Bilinear, deterministic, two-state dynamic causal models were specified for the group of participants that had supra-threshold voxels in all 3 ROIs. The models covered the entire space of possible driving input configurations; the input could be independently provided to any one of the 3 nodes, with the additional constraint that at least one of the nodes should receive it, resulting in 7 possible configurations (Fig. 2). Upon these 7 model families, we also examined modulatory effects exerted on the connections of the network. The modulatory input in the High/Low Emotional Intensity analysis was the High Emotional Intensity regressor. The modulatory input in the Positive/Neutral analysis was the Positive regressor. Again, the modulatory input could be applied to any of the 6 external connections independently, resulting in a total of 64 possible modulatory input configurations. Combined with the 7 model families, the full model space for each participant consisted of 448 models for the High/Low Emotional Intensity Analysis, and 448 models for the Positive/Neutral Analysis. In short, all models had identical endogenous connections, but differed with respect to the region(s) where the driving input was delivered, and the network connections that were targeted by the external modulatory input.

Models families were compared using random-effects Bayesian Model Selection (RFX BMS) (Penny et al., 2010). Models were partitioned into families, and based on the resulting family exceedance probabilities, we assessed the likelihood of different driving input configurations, controlling for effects introduced by the modulatory inputs. RFX BMS provides the means to compute a relative measure of model goodness (Stephan et al., 2010), enabling one to determine the “winning” family of models, i.e., the most likely configuration of driving inputs (assuming there is a clear winner, which may not be always the case). Bayesian Model Averaging (BMA) (Penny et al., 2010) was then applied to the 64

models in the “winning” family of each participant, in order to obtain weighted average model parameters, i.e., the strength of endogenous connections and modulatory effects, where the weight is determined by the posterior model probabilities. The average parameters were entered in a one sample two-tailed *t*-test, and statistical significance was assessed adjusting for multiple comparisons using Bonferroni correction.

### 3. Results

#### 3.1. Behavioral data

Participants diligently performed the AM retrieval task; across all trials, participants only missed 0.19% of the button presses signaling successful construction of a memory associated with the cue. For the subjective ratings given at the end of each trial, the overall mean missing button press rates for emotional intensity, negative affect, and positive affect ratings were 3.13%, 0.65% and 0.26%, respectively. The correlation coefficient (Pearson’s *r*) between the ratings of emotional intensity experienced during the original event given on Day 1 and inside the scanner (Day 2), across all participants, was 0.665 ( $p < 0.0001$ , 95% CI [0.635, 0.692], 1488 datapoints in total); when computed individually for each participant, *r* values were in the range of [0.238, 0.834] (average number of datapoints per participant: 57.2 out of 60). For the ratings of evoked positive affect during memory elaboration, the correlation coefficient across all participants was  $r = 0.775$  ( $p < 0.0001$ , 95% CI [0.755, 0.795], 1532 datapoints in total), with individual values in the range of [0.551, 0.904] (average number of datapoints per participant: 58.9 out of 60). For the ratings of evoked negative affect during memory elaboration, the correlation coefficient across all participants was  $r = 0.768$  ( $p < 0.0001$ , 95% CI [0.747, 0.788], 1526 datapoints in total), with individual values in the range of [0.544, 0.892] (average number of datapoints per participant: 58.7 out of 60). Even though a shorter 4-point scale was employed to collect behavioral ratings in the scanner, these results indicate that behavioral responses were largely consistent with the ratings collected on Day 1, using a 7-point scale. Furthermore, we examined the correlation coefficients between the 3 ratings given inside the scanner. For the emotional intensity and negative affect ratings, *r* values across participants were in the range of [-0.031, 0.544], with

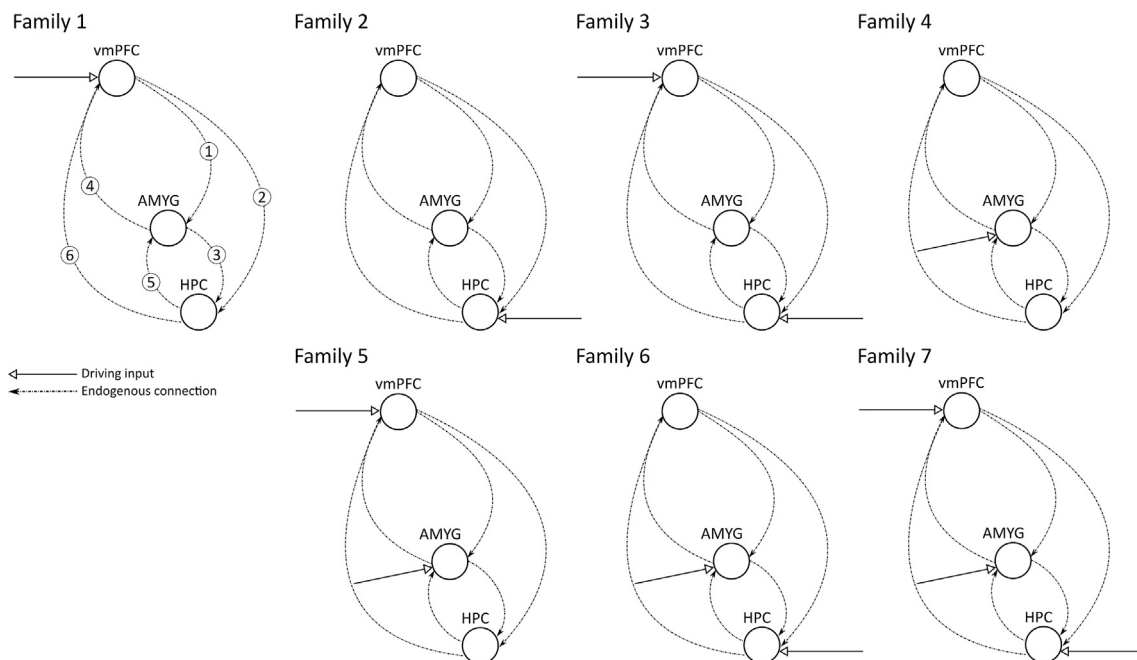


Fig. 2. The 7 model families used in the DCM analyses, determined by the configuration of driving inputs. Models were fully interconnected via 6 intrinsic forward/backward connections.

mean value of 0.382 (average number of trials where both ratings were recorded: 57.2 out of 60). For the emotional intensity and positive affect ratings,  $r$  values were in the range of  $[-0.258, 0.503]$ , with mean value of 0.180 (average number of trials where both ratings were recorded: 57.2 out of 60). For the negative and positive affect ratings,  $r$  values were in the range of  $[-0.807, -0.311]$ , with mean value of  $-0.587$  (average number of trials where both ratings were recorded: 58.7 out of 60). These results suggest that emotional intensity was, at most, only moderately positively correlated with the evoked affect ratings, either negative or positive. In contrast, negative and positive affect ratings were negative correlated at much higher levels, as expected.

Across participants, on average 40% of the trials were rated as Low Emotional Intensity (SD = 13%, range from 12% to 66%), while 60% of the trials were rated as High Emotional Intensity (SD = 13%, range from 34% to 88%). With respect to valence types, on average 29% of the trials were rated as Negative (SD = 7%, range from 13% to 40%), 35% of the trials were rated as Neutral (SD = 13%, range from 11% to 60%), and 37% of the trials were rated as Positive (SD = 9%, range from 24% to 54%). Differences in RT (s) between the Low Emotional Intensity (M = 2.45, SD = 1.20) and High Emotional Intensity (M = 2.38, SD = 1.19) trials failed to reach statistical significance ( $t(25) = 1.949$ ,  $p = 0.063$ ). However, a marginally significant main effect of valence type was detected (Mauchly's test:  $\chi^2(2) = 22.544$ ,  $p < 0.001$ ; rmANOVA:  $F(1.243, 31.073) = 3.773$ ,  $p = 0.053$ ). Exploratory post-hoc tests indicated that participants were in general slightly faster to access a memory in trials judged to be Positive (M = 2.33, SD = 1.21) than Neutral (M = 2.47, SD = 1.34,  $t(25) = 4.12$ ,  $p < 0.005$ , Bonferroni correction for 3 comparisons). All other pairwise comparisons failed to reach significance.

The average evoked positive affect was greater for High Emotional Intensity trials (M = 2.21, SD = 0.23) than for Low Emotional Intensity trials (M = 1.84, SD = 0.40,  $t(25) = 4.53$ ,  $p < 0.001$ ). Likewise, the average evoked negative affect was greater for High Emotional Intensity trials (M = 2.18, SD = 0.27) than for Low Emotional Intensity trials (M = 1.48, SD = 0.27,  $t(25) = 9.61$ ,  $p < 0.001$ ). Differences in average emotional intensity rating across trials of different valence (Negative/Neutral/Positive) were significant (Mauchly's test:  $\chi^2(2) = 12.155$ ,  $p = 0.002$ ; rmANOVA:  $F(1.431, 35.781) = 114.574$ ,  $p < 0.001$ ). Exploratory post-hoc tests indicated that Negative trials received higher emotional intensity ratings (M = 3.26, SD = 0.33) than Neutral (M = 1.92, SD = 0.42,  $t(25) = 12.46$ ,  $p < 0.001$ , Bonferroni correction for 3 comparisons), and Positive trials (M = 3.00, SD = 0.39,  $t(25) = 4.55$ ,  $p < 0.001$ , Bonferroni correction for 3 comparisons). Similarly, emotional intensity ratings for Positive trials were higher than for Neutral trials ( $t(25) = 10.02$ ,  $p < 0.001$ , Bonferroni correction for 3 comparisons).

The mean age of the memories across participants was 4.86 years old (SD = 1.87, range from 2.42 to 8.05). No differences in memory age were detected between Low (M = 4.82, SD = 2.44) and High Emotional Intensity trials (M = 4.84, SD = 1.87,  $t(25) = -0.065$ ,  $p = 0.949$ ), and across different valence types (Mauchly's test:  $\chi^2(2) = 0.220$ ,  $p = 0.896$ ; rmANOVA:  $F(2, 50) = 1.667$ ,  $p = 0.199$ ). In contrast, there were differences in personal significance ratings between Low (M = 1.83, SD = 0.61) and High Emotional Intensity trials (M = 2.87, SD = 0.59,  $t(25) = -12.404$ ,  $p < 0.001$ ), as well as across trials of different valence type (Mauchly's test:  $\chi^2(2) = 1.085$ ,  $p = 0.581$ ; rmANOVA:  $F(2, 50) = 30.916$ ,  $p < 0.001$ ); further exploratory post-hoc tests indicated that the personal significance of events recollected in both Negative (M = 2.74, SD = 0.62) and Positive (M = 2.77, SD = 0.67) trials were given higher ratings than the events recollected in Neutral trials (M = 1.94, SD = 0.63,  $t(25) = 6.42$ ,  $p < 0.00001$ , and  $t(25) = 6.53$ ,  $p < 0.00001$ , respectively, Bonferroni correction for 3 comparisons).

On Day 1, no significant changes were observed in the average Negative or Positive Affect Scores (PANAS) collected before and after the evaluation of phenomenological aspects of the memories used in the scanning experiment (Negative\_before M = 19.27, SD = 5.96;

Negative\_after M = 18.11, SD = 6.92; Positive\_before M = 29.65, SD = 5.99; Positive\_after M = 26.69, SD = 11.11,  $t(25) = 1.169$ ,  $p = 0.253$ , and  $t(25) = 1.734$ ,  $p = 0.095$ , respectively). On Day 2, no changes were detected in the average Negative Affect Score collected before and after scanning (Negative\_before M = 17.04, SD = 4.97; Negative\_after M = 18.73, SD = 5.74,  $t(25) = -1.795$ ,  $p = 0.085$ ); however, the Positive Affect Score after scanning was significantly lower than before scanning (Positive\_before M = 27.04, SD = 7.86; Positive\_after M = 22.42, SD = 8.38,  $t(25) = 4.512$ ,  $p < 0.001$ ).

### 3.2. DCM

In order to locate the clusters within the vmPFC, hippocampus and amygdala from where the timeseries would be extracted for each participant, we first determined the group-level MNI peak voxel coordinates in each one of the ROIs to guide the search. Before determining the group-level peak voxels to be used in the emotional intensity DCM analysis, we examined the results of the contrast [*High Emotional Intensity - Low Emotional Intensity*], in order to evaluate the effectiveness of the manipulation (Table 1); clusters of activity were found in the vmPFC and left amygdala. The peak voxel coordinates for the emotional intensity DCM analysis were obtained using the contrast [*High Emotional Intensity + Low Emotional Intensity*]; they were vmPFC: MNI (-4, 40, -14); left hippocampus: MNI (-22, -14, -18); left amygdala: MNI (-22, -12, -14).

Though we initially planned to analyze effective connectivity effects for both evoked negative and positive affects, when assessing the effectiveness of the manipulation using the contrast [*Negative - Neutral*], no significant effects were observed in the voxels within the 3 ROIs (Table 1). Further inspection indicated that none of the ROIs displayed parametric modulation effects associated with negative affect ratings (see Supplementary Material), when controlling for emotional intensity, suggesting that with regard to evoked negative affect, the manipulation had not been entirely effective. In contrast, results from the contrast [*Positive - Neutral*] indicated the presence of effects in all 3 ROIs (Table 1). Furthermore, parametric modulation effects directly proportional with the positive affect ratings (controlling for emotional intensity) were observed in the vmPFC and hippocampus (Supplementary Material). Given these findings, we decided to focus the valence DCM analysis only on the modulatory effects of evoked positive affect. The peak voxel coordinates for the positive affect DCM analysis were obtained using the contrast [*Positive + Neutral*]; they were vmPFC: MNI (-4, 40, -14); left hippocampus: MNI (-22, -18, -16); left amygdala: MNI (-16, -10, -14).

After attempting to extract timeseries data from all regions and all participants, analyses were performed on the cohort of participants where valid timeseries could be extracted for all 3 ROIs: all participants for the High/Low Emotional Intensity analysis, and 24 participants for the Positive/Neutral analysis (one male and one female participant had to be excluded because no supra-threshold voxels were found in the left amygdala).

Following computation of the full model space for the participants in each cohort, a RFX BMS was performed to compare the model families, allowing us to select the family whose likelihood (exceedance probability) was larger than the other tested families, as well as to examine the probability of a family of models generating the data of a randomly chosen subject (expected posterior probability). Models were separated into families according to the nodes receiving the driving input. Both the results of the emotional intensity RFX BMS, and the valence RFX BMS clearly favored the family of models where the driving input was only applied to the vmPFC, with exceedance probabilities of 0.9927 and 0.9903, respectively, and expected posterior probabilities of 0.5706 and 0.5338, respectively.

After determining that the family of models where the driving input was assigned exclusively to the vmPFC was the "winner", we sought to verify the nature of the endogenous (intrinsic) connections in that model

**Table 1**

Results for the contrasts [High Emotional Intensity – Low Emotional Intensity], [Negative – Neutral], and [Positive – Neutral]. Peaks voxels within each cluster are shown in MNI coordinates. P-values corrected for multiple comparisons (family-wise error correction within the small-volume determined by the respective mask). Supra-threshold voxels ( $p < 0.05$ ) in boldface. All masks derived from the Harvard-Oxford atlas. Masks for the hippocampus (HPC) and amygdala (AMYG) were thresholded (60) to minimize overlap. Activity in the vmPFC was examined using the “Frontal Medial Cortex” mask.

		x	y	z	Z	P-value
<i>High – Low Emotional Intensity</i>	<b>vmPFC</b>	<b>0</b>	<b>30</b>	<b>-10</b>	<b>4.70</b>	<b>0.002</b>
	L HPC	-30	-16	-14	2.99	0.118
	<b>L AMYG</b>	<b>-24</b>	<b>-10</b>	<b>-12</b>	<b>3.45</b>	<b>0.016</b>
<i>Negative – Neutral</i>	vmPFC	6	58	2	1.74	0.993
	L HPC	-	-	-	-	-
	L AMYG	-24	-10	-12	2.77	0.096
<i>Positive – Neutral</i>	<b>vmPFC</b>	<b>2</b>	<b>58</b>	<b>2</b>	<b>4.02</b>	<b>0.029</b>
	<b>L HPC</b>	<b>-32</b>	<b>-30</b>	<b>-8</b>	<b>3.4</b>	<b>0.037</b>
	<b>L AMYG</b>	<b>-24</b>	<b>-12</b>	<b>-12</b>	<b>3.27</b>	<b>0.025</b>

family, i.e., the baseline connectivity strengths of the connections, as well as the effect of modulatory inputs (associated with the experimental manipulations) onto the network connections. The total connectivity strength associated with an experimental manipulation is the total sum of the endogenous connectivity with additional effects introduced by the modulatory inputs. Parameters of the models in the “winning” family were averaged using BMA, within each participant, and then tested for consistency of effects across participants. Results from the emotional intensity DCM are summarized in Table 2 and Fig. 3A. They indicated the existence of positive endogenous connections from the vmPFC to the amygdala and hippocampus, and from the amygdala to the hippocampus, during memory elaboration. Moreover, positive effects associated with the emotional intensity modulatory input (High Emotional Intensity) were observed in the connection linking the vmPFC to the hippocampus. Results from the positive affect DCM are summarized in Table 3 and Fig. 3B. They indicated the existence of positive endogenous connections from the vmPFC to the hippocampus, and from the amygdala to the hippocampus. Furthermore, positive effects associated with the positive affect modulatory input (Positive) were observed in the connection linking the vmPFC to the hippocampus.

**4. Discussion**

The present results indicate that the vmPFC is a driver of hippocampal activity during the elaboration of autobiographical memories, suggesting that the vmPFC has a central role among the nodes in the putative AM retrieval network. Participants were asked to elaborate on personal memories in the scanner, after being cued using preselected memory-triggers of various types of valence and degrees of emotional intensity. In our DCM analyses, the external input that directly drives the activity of the network nodes, i.e., the driving input, consisted of an all-inclusive

series of memory elaboration phases, in effect, describing the periods of time that participants actively engaged in reliving personal memories. Our results clearly favored the family of models where the driving input was applied exclusively to the vmPFC, suggesting that during the elaboration of personal memories, the vmPFC occupies a position from where it can directly influence the activity in the amygdala and hippocampus, rather than the other way around. Inspection of the endogenous connections of the models in the winning family, which reflect the underlying intrinsic strength of the links connecting the nodes in the model, further indicated the modulation of the hippocampus by the vmPFC: results of the DCM analysis focusing on emotional intensity revealed that activity in the amygdala and the hippocampus was majorly driven by the vmPFC (Table 2, Endogenous connections). Results of the DCM analysis focusing on positive affect depicted a similar picture; even though the link from the vmPFC to the amygdala failed to reach statistical significance after correcting for multiple comparisons, a positive endogenous connection from the vmPFC to the hippocampus was observed (Table 3, Endogenous connections). Positive endogenous amygdala to hippocampus connections were also found in both emotional intensity and positive affect DCM analyses, though the strength of that connection based on model estimates was approximately 5 and 7 times smaller than the vmPFC to hippocampus connection, respectively, suggesting that, indeed, it is the vmPFC that primarily drives hippocampal activity during memory elaboration. It is worth noting that the absence of a vmPFC to amygdala endogenous connection in the results from the positive affect DCM is likely to be a statistical thresholding artefact, since the amygdala to hippocampus connection was still found to be significant. Taken as a whole, these results reinforce the notion that with respect to the direction of information flow, the vmPFC acts as a source to the amygdala and hippocampus, i.e., both subcortical structures are positioned further downstream relative to the vmPFC.

Our results are also in line with studies that have employed machine-learning based multivariable pattern analysis (MVPA) (Chadwick et al., 2012; Haynes and Rees, 2006) to successfully classify autobiographical memories based on their recency from brain activity recorded from the vmPFC and hippocampus (Bonnici et al., 2012; Bonnici and Maguire, 2018). Such studies suggest that information about AMs are well represented in those areas, as well as in other regions of the putative AM retrieval network (Rissman et al., 2016). Interestingly, Bonnici et al. (2012) and Bonnici and Maguire (2018) have shown that when using fMRI data from the vmPFC or posterior hippocampus, remote memories (2 years old) can be better discerned than more recent memories (2 weeks old), consistent with models that attribute a critical role to the vmPFC during memory consolidation (Nieuwenhuis and Takashima, 2011). Taken together, the picture that emerges depicts the vmPFC as serving as a major substrate of remote AM representations; the current results would additionally suggest that the vmPFC channels that information to the hippocampus during the elaboration of personal memories. Though it may appear initially surprising that the vmPFC is in an upstream position relative to the hippocampus, it has been shown, albeit in a different context, that the vmPFC modulates theta oscillations in the

**Table 2**

Network parameter estimates from the emotional intensity DCM analysis across 26 participants. \* Significant coupling parameters at  $p < 0.05$  (Bonferroni).

		Mean	S.D.	95% C.I.	t-value (t(25))	P-value
Endogenous connections	vmPFC → Amygdala	0.14*	0.04	0.04 to 0.23	3.03	5.5 1e-3
	vmPFC → Hippocampus	0.26*	0.04	0.18 to 0.35	6.32	1.30 1e-6
	Amygdala → Hippocampus	0.05*	0.05	0.03 to 0.07	4.50	1.35 1e-4
	Amygdala → vmPFC	0.02	0.05	-0.01 to 0.05	1.41	0.17
	Hippocampus → Amygdala	0.04	0.05	0.01 to 0.07	2.78	0.01
	Hippocampus → vmPFC	0.03	0.05	-0.01 to 0.08	1.60	0.12
Modulatory inputs	vmPFC → Amygdala	0.14	0.08	-0.02 to 0.31	1.81	0.08
	vmPFC → Hippocampus	0.31*	0.07	0.17 to 0.45	4.65	9.17 1e-5
	Amygdala → Hippocampus	0.02	0.06	0.00 to 0.04	2.58	0.02
	Amygdala → vmPFC	-0.01	0.07	-0.05 to 0.02	-0.64	0.53
	Hippocampus → Amygdala	0.02	0.07	-0.01 to 0.06	1.21	0.24
	Hippocampus → vmPFC	-0.00	0.08	-0.09 to 0.08	-0.11	0.92

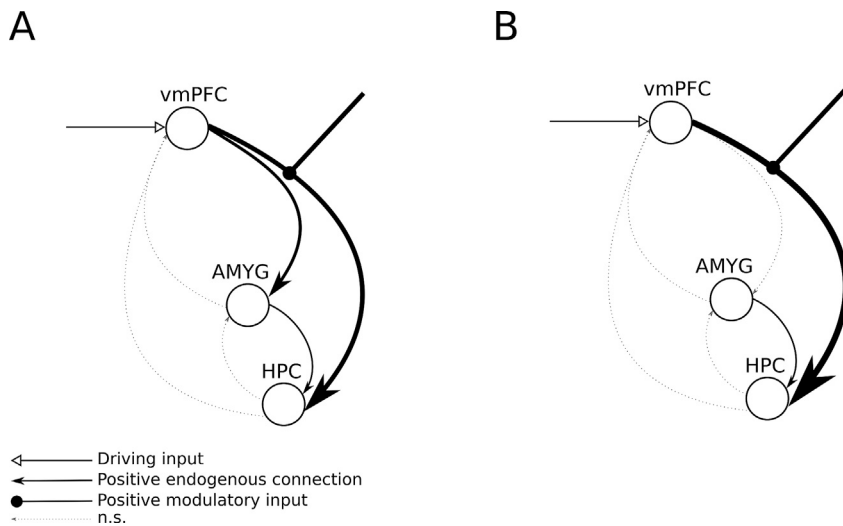


**Fig. 3.** Mean network parameters of the models in the winning family computed using BMA. Results from the emotional intensity DCM indicated the existence of positive endogenous connections from the vmPFC to the amygdala (AMYG) and hippocampus (HPC), as well as from AMYG to HPC. The vmPFC to HPC effective connectivity was enhanced in trials where participants elaborated memories of events deemed to be of high emotional intensity (A). Results from the positive affect DCM indicated the existence of positive endogenous connections from the vmPFC to the HPC (but not AMYG), as well as from AMYG to HPC. Similarly, the vmPFC to HPC effective connectivity was enhanced during trials that evoked positive affect (B). In both cases, the driving input in the winning family of models only served the vmPFC. The relative magnitude of endogenous and modulatory connections is reflected in the width of the corresponding arrow.

hippocampus, assessed using DCM on magnetoencephalography (MEG) data, in a task involving match-mismatch detection on pairs of visual stimuli (Garrido et al., 2015), suggesting that during novelty processing, it is the vmPFC that drives the activity in the hippocampus.

The same hierarchy between the vmPFC and hippocampus was highlighted by the findings regarding modulatory effects associated with emotional intensity and evoked positive affect in the connections of the triadic network. Results of the DCM focusing on emotional intensity showed that the vmPFC to hippocampus effective connectivity increased when participants recollected episodes that were highly emotionally intense (the High Emotional Intensity trials) (Table 2, Modulatory inputs). Because trials of different valence types were mixed within the High Emotional Intensity trials, this effect may be independent of the valence of the evoked affect. In a similar manner, the results of the DCM analysis focusing on positive affect indicated the existence of a positive modulatory effect on the vmPFC to hippocampus connection during the elaboration of memories that more strongly evoked positive affect (the Positive trials), across different degrees of emotional intensity (Table 3, Modulatory inputs). Results from a parametric modulation analysis (Supplementary Material) showed that all major nodes in the putative AM retrieval network displayed increases in activity during the elaboration of autobiographical memories, but only the amygdala, hippocampus, vmPFC, precuneus and PCC were modulated by either the emotional intensity ratings, evoked positive affect ratings, or both. Interestingly, and in line with past reports (Lin et al., 2016; Roy et al., 2012; Speer et al., 2014; Winecoff et al., 2013), activity in the vmPFC during memory elaboration increased proportionally to subjective ratings of emotional intensity and evoked positive affect (controlling for emotional intensity). Together with the DCM analyses results, these results suggest that information about affective aspects of personal

memories is indeed majorly processed and/or represented in the vmPFC, and moreover, that the vmPFC relays that information to the hippocampus, and the amygdala, during memory elaboration.

All in all, the current results underscore the possibility that the vmPFC plays two crucial roles during the elaboration of AMs in general, and positive and emotional memories in particular. Reminiscing about a personal memory primarily drives the activity of the vmPFC, and from there, activity in the amygdala and hippocampus are enhanced. Furthermore, during the elaboration of memories of personal episodes associated with greater emotional intensity or memories that evoke stronger positive affect, the influence of the vmPFC on the hippocampus is enhanced. Thus, the vmPFC appears to have a central role not only in supporting the representation of AMs, but also in providing that information to drive hippocampal activity during memory elaboration, while at the same time, supporting the generation of affective responses that originate from information associated with such memories (Roy et al., 2012).

Most remarkably, the current results suggest a hierarchical organization that places the vmPFC in a superior position relative to the hippocampus, in line with a model recently proposed by McCormick et al. (2017). According to that model, a major role of the vmPFC would be to guide processes associated with the construction of coherent sequences of mental scenes in the hippocampus, not only during autobiographical memory retrieval, but also during other capacities thought to be supported by a highly overlapping network of brain regions, such as episodic future thinking and navigation. The hierarchical relationship between the vmPFC and hippocampus is postulated to become more evident during the retrieval of remote memories than recent ones, since they have been associated with greater involvement of the vmPFC (Bonnici et al., 2012; Bonnici and Maguire, 2018). Using standards adopted in

**Table 3**

Network parameter estimates from the positive affect DCM analysis across 24 participants. \*Significant coupling parameters at  $p < 0.05$  (Bonferroni).

		Mean	S.D.	95% C.I.	t-value (t(23))	P-value
Endogenous connections	vmPFC → Amygdala	0.08	0.05	0.02 to 0.14	2.65	0.01
	vmPFC → Hippocampus	0.21*	0.04	0.12 to 0.30	4.90	5.93 1e-5
	Amygdala → Hippocampus	0.03*	0.05	0.01 to 0.06	3.12	4.90 1e-3
	Amygdala → vmPFC	0.03	0.05	-0.01 to 0.07	1.61	0.12
	Hippocampus → Amygdala	0.02	0.05	0.00 to 0.05	2.13	0.04
	Hippocampus → vmPFC	0.03	0.05	-0.01 to 0.06	1.45	0.16
Modulatory inputs	vmPFC → Amygdala	0.17	0.09	0.00 to 0.33	2.14	0.04
	vmPFC → Hippocampus	0.30*	0.08	0.15 to 0.45	4.18	3.58 1e-4
	Amygdala → Hippocampus	0.02	0.07	0.00 to 0.04	2.47	0.02
	Amygdala → vmPFC	0.05	0.08	-0.01 to 0.11	1.57	0.13
	Hippocampus → Amygdala	0.02	0.08	-0.02 to 0.06	1.20	0.24
	Hippocampus → vmPFC	0.04	0.08	-0.02 to 0.09	1.46	0.16

other studies, the memories relived by our participants are clearly not recent, making our results consistent with the prediction that when recalling remote memories, activity in the hippocampus should be predominantly driven by the vmPFC. Though the vmPFC has been typically associated with affective processes, our results suggest that the vmPFC may play a more fundamental role that goes beyond shaping affective responses associated with AMs. Following successful memory construction, the vmPFC appears to integrate information associated with the accessed memory to further guide and constrain hippocampal processes occurring during episodic memory elaboration. Though the results of our study alone cannot completely confirm the model put forward by McCormick et al. (2017), the possibility is intriguing and deserves further examination.

In the light of memory deficiencies presented by patients with lesions in the vmPFC, most notably confabulation (Bertossi et al., 2016; Ghosh et al., 2014; Spalding et al., 2015), is it possible to more specifically characterize the nature of the information passed by the vmPFC to the hippocampus, beyond information regarding affective aspects of AMs? One possibility is that such vmPFC signals are primarily related to schemas, i.e., regularities extracted from prior knowledge and across experiences that facilitate and bias the encoding, consolidation and retrieval of information in the form of episodic memories and knowledge (Ghosh and Gilboa, 2014; Gilboa and Marlatte, 2017; van Kesteren et al., 2012). Confabulation is observed in some vmPFC patients, and it is characterized by the failure to monitor and detect erroneous memories. That deficit has been attributed to an inability to suppress irrelevant schemas, which leads to the retrieval of false memories and the belief that they are authentic. One possibility suggested by the current results is that during episodic memory elaboration, the signals from the vmPFC also serve to organize the elements associated with the recalled memory based on existing memory schemas. That information would be fed to the hippocampus, which would then carry on processes related to memory elaboration, such as scene construction, along the lines of the model proposed in (McCormick et al., 2017). Interestingly, the reference voxel in the left hippocampus for both DCM analyses was located in the anterior hippocampus, a region that has been postulated to be heavily involved with scene construction processes (Zeidman and Maguire, 2016). Taken more broadly, the current results add to the mounting evidence indicating that prefrontal cortex-hippocampal interactions are key in a number of cognitive capacities (Gluth et al., 2015; Preston and Eichenbaum, 2013; Rubin et al., 2014).

Finally, this study has several caveats. One critical limitation of the DCM analyses presented here is that they obviously only offer a partial view of processes that are likely to involve the coordination of a much wider network. Here, effective connectivity was examined only within the vmPFC-hippocampus-amygdala network; the inclusion of additional brain regions, such as the precuneus and the PCC, both of which, like the vmPFC, showed enhanced activation during the elaboration of emotional and positive AMs (Supplementary Material), should provide a more complete view of the interactions occurring within the AM retrieval network during the various stages of memory recall. It may be found, for example, that an ensemble of regions further upstream are the originators of the information passed to the hippocampus via the vmPFC during memory elaboration, or contrarily, that the precuneus and/or PCC are influenced by the vmPFC via the hippocampus or through alternative pathways.

Also, it is important to note that the direction of information flow in the endogenous connections of the triadic network characterized by the DCM analyses results is specific to the memory elaboration phase. There is evidence suggesting that in the initial stages of AM retrieval, and episodic future thinking, memory processes are centered in the hippocampus (Campbell et al., 2017; Daselaar et al., 2008; McCormick et al., 2015; Preston and Eichenbaum, 2013). If that is the case, our results would suggest that the flow of information between the vmPFC and hippocampus changes directions when transitioning from the *construction* to the *elaboration phase* during AM retrieval. An alternative hypothesis

would be that the vmPFC also initiates memory retrieval processes (McCormick et al., 2017), in which case we should observe a similar hierarchical structure between the vmPFC to the hippocampus during memory construction. That remains to be clarified by future studies, perhaps combining different neuroimaging modalities, such as MEG, e.g., (Garrido et al., 2015). Also, it is important to keep in mind that the DCM analysis here was based on an indirect, low-temporal resolution measure of brain activity, with all the merits and limitations provided by the BOLD signal.

Another limitation is that we were unable to thoroughly examine the imaging data from the perspective of evoked negative affect, even though we preselected verbal cues that should be associated with negative memories, judging from ratings collected before scanning. It remains to be verified whether our statistical tests lacked power due to, e.g., lower engagement of participants during the negative trials, or if there are fundamental differences in the neuropsychological processes involved in the elaboration of negative AMs. Of note, we purposefully treated negative and positive affect independently by separately collecting negative and positive affect ratings, and allowing both types of affect to coexist at the same time. This approach allows one to more flexibly assess both valence-general and valence-specific effects, since it does not assume a priori that both types of hedonic valence are opposite ends of a single dimension, nor that they are primarily supported by a common neural basis (Lindquist et al., 2015).

It also remains to be established how the network subserving episodic memory retrieval is affected by differences in vividness levels experienced during the elaboration of AMs, since memories stemming from highly arousing events or memories that evoke greater levels of positive or negative affect are arguably associated with more vivid recollections. Though we did not directly ask our participants to evaluate the imagery vividness experienced inside the scanner, we collected data that could serve as a composite index of vividness, i.e., questions 13, 14, 15 from (Talarico et al., 2004). Vividness has been shown to modulate activity in the hippocampus (Addis et al., 2004), and our preliminary results using the current dataset are consistent with that finding, though no modulatory effects were observed in the vmPFC or amygdala (Nawa and Ando, 2018). Further advancing this line of research will help better characterize the effects of this important phenomenological aspect of AMs.

One final limitation is that we restricted analysis to regions in the left hemisphere. Though AM retrieval processes have been reported predominantly on left-lateralized regions, the extent of that lateralization still remains to be confirmed.

## Declaration of interest

None.

## Acknowledgements

We would like to thank three anonymous reviewers for their helpful and enlightening comments on previous versions of this manuscript. We would also like to thank M. Delgado for sharing material used to help participants remember the personal memories used in the experiments, and M. Fastenrath for advice on the nuts and bolts of dynamic causal modeling. We are particularly indebted to the imaging staff at the Center for Neural and Information Neural Networks for their invaluable and often ingenious help running the imaging experiments. This work was supported by the Japan Society for the Promotion of Science under a Grant-in-Aid for Scientific Research (JSPS KAKENHI grant number JP17K00220 to NEN). The funding source was not involved in any stage of the research described in this article.

## Appendix A. Supplementary data

Supplementary data to this article can be found online at <https://doi.org/10.1016/j.neuroimage.2019.01.042>.

## References

- Addis, D.R., Moscovitch, M., Crawley, A.P., McAndrews, M.P., 2004. Recollective qualities modulate hippocampal activation during autobiographical memory retrieval. *Hippocampus* 14, 752–762. <https://doi.org/10.1002/hipo.10215>.
- Addis, D.R., Wong, A.T., Schacter, D.L., 2007. Remembering the past and imagining the future: common and distinct neural substrates during event construction and elaboration. *Neuropsychologia* 45, 1363–1377. <https://doi.org/10.1016/j.neuropsychologia.2006.10.016>.
- Anderson, A.K., Wais, P.E., Gabrieli, J.D.E., 2006. Emotion enhances remembrance of neutral events past. *Proc. Natl. Acad. Sci. U.S.A.* 103, 1599–1604. <https://doi.org/10.1073/pnas.0506308103>.
- Beck, A.T., Steer, R.A., Brown, G., 1996. *Beck Depression Inventory Manual*. The Psychological Corporation.
- Benoit, R.G., Schacter, D.L., 2015. Specifying the core network supporting episodic simulation and episodic memory by activation likelihood estimation. *Neuropsychologia* 75, 450–457. <https://doi.org/10.1016/j.neuropsychologia.2015.06.034>.
- Benoit, R.G., Szpunar, K.K., Schacter, D.L., 2014. Ventromedial prefrontal cortex supports affective future simulation by integrating distributed knowledge. *Proc. Natl. Acad. Sci. U.S.A.* 111, 16550–16555. <https://doi.org/10.1073/pnas.1419274111>.
- Bertossi, E., Tesini, C., Cappelli, A., Ciaramelli, E., 2016. Ventromedial prefrontal damage causes a pervasive impairment of episodic memory and future thinking. *Neuropsychologia* 90, 12–24. <https://doi.org/10.1016/j.neuropsychologia.2016.01.034>.
- Bird, C.M., Burgess, N., 2008. The hippocampus and memory: insights from spatial processing. *Nat. Rev. Neurosci.* 9, 182–194. <https://doi.org/10.1038/nrn2335>.
- Bloise, S.M., Johnson, M.K., 2007. Memory for emotional and neutral information: gender and individual differences in emotional sensitivity. *Memory* 15, 192–204. <https://doi.org/10.1080/09658210701204456>.
- Bonnici, H.M., Chadwick, M.J., Lutti, A., Hassabis, D., Weiskopf, N., Maguire, E.A., 2012. Detecting representations of recent and remote autobiographical memories in vmPFC and hippocampus. *J. Neurosci.* 32, 16982–16991. <https://doi.org/10.1523/JNEUROSCI.2475-12.2012>.
- Bonnici, H.M., Maguire, E.A., 2018. Two years later – revisiting autobiographical memory representations in vmPFC and hippocampus. *Neuropsychologia* 110, 159–169. <https://doi.org/10.1016/j.neuropsychologia.2017.05.014>.
- Buchanan, T.W., 2007. Retrieval of emotional memories. *Psychol. Bull.* 133, 761–779. <https://doi.org/10.1037/0033-2909.133.5.761>.
- Buchanan, T.W., Tranel, D., Adolphs, R., 2005. Emotional autobiographical memories in amnesic patients with medial temporal lobe damage. *J. Neurosci.* 25, 3151–3160. <https://doi.org/10.1523/JNEUROSCI.4735-04.2005>.
- Buckner, R.L., Carroll, D.C., 2007. Self-projection and the brain. *Trends Cognit. Sci. (Regul. Ed.)* 11, 49–57. <https://doi.org/10.1016/j.tics.2006.11.004>.
- Cabeza, R., St Jacques, P.L., 2007. Functional neuroimaging of autobiographical memory. *Trends Cognit. Sci. (Regul. Ed.)* 11, 219–227. <https://doi.org/10.1016/j.tics.2007.02.005>.
- Cahill, L., Babinsky, R., Markowitsch, H.J., McGaugh, J.L., 1995. The amygdala and emotional memory. *Nature* 377, 295–296. <https://doi.org/10.1038/377295a0>.
- Cahill, L., Haier, R.J., Fallon, J., Alkire, M.T., Tang, C., Keator, D., Wu, J., McGaugh, J.L., 1996. Amygdala activity at encoding correlated with long-term, free recall of emotional information. *Proc. Natl. Acad. Sci. U.S.A.* 93, 8016–8021.
- Cahill, L., Prins, B., Weber, M., McGaugh, J.L., 1994. Beta-adrenergic activation and memory for emotional events. *Nature* 371, 702–704. <https://doi.org/10.1038/371702a0>.
- Campbell, K.L., Madore, K.P., Benoit, R.G., Thakral, P.P., Schacter, D.L., 2017. Increased hippocampus to ventromedial prefrontal connectivity during the construction of episodic future events. *Hippocampus* 45, 1363–1365. <https://doi.org/10.1002/hipo.22812>.
- Chadwick, M.J., Bonnici, H.M., Maguire, E.A., 2012. Decoding information in the human hippocampus: a user's guide. *Neuropsychologia* 50, 3107–3121. <https://doi.org/10.1016/j.neuropsychologia.2012.07.007>.
- Conway, M.A., Pleydell-Pearce, C.W., 2000. The construction of autobiographical memories in the self-memory system. *Psychol. Rev.* 107, 261–288.
- Conway, M.A., Turk, D.J., Miller, S.L., Logan, J., Nebes, R.D., Meltzer, C.C., Becker, J.T., 1999. A positron emission tomography (PET) study of autobiographical memory retrieval. *Memory* 7, 679–703. <https://doi.org/10.1080/096582199387805>.
- Daselaar, S.M., Rice, H.J., Greenberg, D.L., Cabeza, R., LaBar, K.S., Rubin, D.C., 2008. The spatiotemporal dynamics of autobiographical memory: neural correlates of recall, emotional intensity, and reliving. *Cerebr. Cortex* 18, 217–229. <https://doi.org/10.1093/cercor/bhm048>.
- Delgado, M.R., Beer, J.S., Fellows, L.K., Huettel, S.A., Platt, M.L., Quirk, G.J., Schiller, D., 2016. Viewpoints: dialogues on the functional role of the ventromedial prefrontal cortex. *Nat. Neurosci.* 19, 1545–1552. <https://doi.org/10.1038/nn.4438>.
- Denburg, N.L., Buchanan, T.W., Tranel, D., Adolphs, R., 2003. Evidence for preserved emotional memory in normal older persons. *Emotion* 3, 239–253. <https://doi.org/10.1037/1528-3542.3.3.239>.
- Desikan, R.S., Ségonne, F., Fischl, B., Quinn, B.T., Dickerson, B.C., Blacker, D., Buckner, R.L., Dale, A.M., Maguire, R.P., Hyman, B.T., Albert, M.S., Killiany, R.J., 2006. An automated labeling system for subdividing the human cerebral cortex on MRI scans into gyral based regions of interest. *Neuroimage* 31, 968–980. <https://doi.org/10.1016/j.neuroimage.2006.01.021>.
- Dolcos, F., LaBar, K.S., Cabeza, R., 2005. Remembering one year later: role of the amygdala and the medial temporal lobe memory system in retrieving emotional memories. *Proc. Natl. Acad. Sci. U.S.A.* 102, 2626–2631. <https://doi.org/10.1073/pnas.0409848102>.
- Dolcos, F., LaBar, K.S., Cabeza, R., 2004. Interaction between the amygdala and the medial temporal lobe memory system predicts better memory for emotional events. *Neuron* 42, 855–863.
- Eichenbaum, H., 2017. Prefrontal–hippocampal interactions in episodic memory. *Nat. Rev. Neurosci.* 18, 547–558. <https://doi.org/10.1038/nrn.2017.74>.
- Fastenrath, M., Coynell, D., Spalek, K., Milnik, A., Gschwind, L., Rozenzdaal, B., Papassotiropoulos, A., de Quervain, D.J.F., 2014. Dynamic modulation of amygdala–hippocampal connectivity by emotional arousal. *J. Neurosci.* 34, 13935–13947. <https://doi.org/10.1523/JNEUROSCI.0786-14.2014>.
- Fischl, B., Salat, D.H., Busa, E., Albert, M., Dieterich, M., Haselgrove, C., van der Kouwe, A., Killiany, R., Kennedy, D.P., Klavness, S., Montillo, A., Makris, N., Rosen, B., Dale, A.M., 2002. Whole brain segmentation: automated labeling of neuroanatomical structures in the human brain. *Neuron* 33, 341–355.
- Ford, J.H., Morris, J.A., Kensinger, E.A., 2014. Effects of emotion and emotional valence on the neural correlates of episodic memory search and elaboration. *J. Cognit. Neurosci.* 26, 825–839. [https://doi.org/10.1162/jocn\\_a.00529](https://doi.org/10.1162/jocn_a.00529).
- Friston, K.J., 2009. Causal modelling and brain connectivity in functional magnetic resonance imaging. *PLoS Biol.* 7, e33. <https://doi.org/10.1371/journal.pbio.1000033>.
- Friston, K.J., Harrison, L., Penny, W.D., 2003. Dynamic causal modelling. *Neuroimage* 19, 1273–1302.
- Gardini, S., Cornoldi, C., De Beni, R., Venneri, A., 2006. Left mediotemporal structures mediate the retrieval of episodic autobiographical mental images. *Neuroimage* 30, 645–655. <https://doi.org/10.1016/j.neuroimage.2005.10.012>.
- Garrido, M.I., Barnes, G.R., Kumaran, D., Maguire, E.A., Dolan, R.J., 2015. Ventromedial prefrontal cortex drives hippocampal theta oscillations induced by mismatch computations. *Neuroimage* 120, 362–370. <https://doi.org/10.1016/j.neuroimage.2015.07.016>.
- Ghosh, V.E., Gilboa, A., 2014. What is a memory schema? A historical perspective on current neuroscience literature. *Neuropsychologia* 53, 104–114. <https://doi.org/10.1016/j.neuropsychologia.2013.11.010>.
- Ghosh, V.E., Moscovitch, M., Melo Colella, B., Gilboa, A., 2014. Schema representation in patients with ventromedial PFC lesions. *J. Neurosci.* 34, 12057–12070. <https://doi.org/10.1523/JNEUROSCI.0740-14.2014>.
- Gilboa, A., 2004. Autobiographical and episodic memory—one and the same? Evidence from prefrontal activation in neuroimaging studies. *Neuropsychologia* 42, 1336–1349. <https://doi.org/10.1016/j.neuropsychologia.2004.02.014>.
- Gilboa, A., Marlatte, H., 2017. Neurobiology of schemas and schema-mediated memory. *Trends Cognit. Sci. (Regul. Ed.)* 21, 618–631. <https://doi.org/10.1016/j.tics.2017.04.013>.
- Gilmore, A.W., Nelson, S.M., Chen, H.-Y., McDermott, K.B., 2018. Task-related and resting-state fMRI identify distinct networks that preferentially support remembering the past and imagining the future. *Neuropsychologia* 110, 180–189. <https://doi.org/10.1016/j.neuropsychologia.2017.06.016>.
- Glasser, M.F., Coalson, T.S., Robinson, E.C., Hacker, C.D., Harwell, J., Yacoub, E.S., Ugurbil, K., Andersson, J.L.R., Beckmann, C.F., Jenkinson, M., Smith, S.M., Van Essen, D.C., 2016. A multi-modal parcellation of human cerebral cortex. *Nature* 536, 171–178. <https://doi.org/10.1038/nature18933>.
- Gluth, S., Sommer, T., Rieskamp, J., Büchel, C., 2015. Effective connectivity between Hippocampus and ventromedial prefrontal cortex controls preferential choices from memory. *Neuron* 86, 1078–1090. <https://doi.org/10.1016/j.neuron.2015.04.023>.
- Hamann, S., Ely, T.D., Grafton, S.T., Kilts, C.D., 1999. Amygdala Activity Related to Enhanced Memory for Pleasant and Aversive Stimuli, vol. 2. *Nature Publishing Group*, pp. 289–293. <https://doi.org/10.1038/6404>.
- Hassabis, D., Maguire, E.A., 2009. The construction system of the brain. *Phil. Trans. Biol. Sci.* 364, 1263–1271. <https://doi.org/10.1098/rstb.2008.0296>.
- Haynes, J.-D., Rees, G., 2006. Decoding mental states from brain activity in humans. *Nat. Rev. Neurosci.* 7, 523–534. <https://doi.org/10.1038/nrn1931>.
- Janak, P.H., Tye, K.M., 2015. From circuits to behaviour in the amygdala. *Nature* 517, 284–292. <https://doi.org/10.1038/nature14188>.
- Kim, M.J., Whalen, P.J., 2009. The structural integrity of an amygdala–prefrontal pathway predicts trait anxiety. *J. Neurosci.* 29, 11614–11618. <https://doi.org/10.1523/JNEUROSCI.2335-09.2009>.
- Kojima, M., Furukawa, T.A., Takahashi, H., Kawai, M., Nagaya, T., Tokudome, S., 2002. Cross-cultural validation of the Beck depression inventory-II in Japan. *Psychiatr. Res.* 110, 291–299.
- la Vega, de, A., Chang, L.J., Banich, M.T., Wager, T.D., Yarkoni, T., 2016. Large-scale meta-analysis of human medial frontal cortex reveals tripartite functional organization. *J. Neurosci.* 36, 6553–6562. <https://doi.org/10.1523/JNEUROSCI.4402-15.2016>.
- LaBar, K.S., Cabeza, R., 2006. *Cognitive Neuroscience of Emotional Memory*, vol. 7. *Nature Publishing Group*, pp. 54–64. <https://doi.org/10.1038/nrn1825>.
- Leal, S.L., Tighe, S.K., Jones, C.K., Yassa, M.A., 2014. Pattern separation of emotional information in hippocampal dentate and CA3. *Hippocampus* 24, 1146–1155. <https://doi.org/10.1002/hipo.22298>.
- Lin, W.-J., Horner, A.J., Burgess, N., 2016. Ventromedial prefrontal cortex, adding value to autobiographical memories. *Sci. Rep.* 1–10. <https://doi.org/10.1038/srep28630>.
- Lindquist, K.A., Satpute, A.B., Wager, T.D., Weber, J., Barrett, L.F., 2015. The brain basis of positive and negative affect: evidence from a meta-analysis of the human neuroimaging literature. *Cerebr. Cortex* 1–13. <https://doi.org/10.1093/cercor/bhv001>.
- Mackey, S., Petrides, M., 2014. Architecture and morphology of the human ventromedial prefrontal cortex. *Eur. J. Neurosci.* 40, 2777–2796. <https://doi.org/10.1111/ejn.12654>.

- Maguire, E.A., 2001. Neuroimaging studies of autobiographical event memory. *Philos. Trans. R. Soc. Lond. B Biol. Sci.* 356, 1441–1451. <https://doi.org/10.1098/rstb.2001.0944>.
- Maguire, E.A., Frith, C.D., 2003. Lateral asymmetry in the hippocampal response to the remoteness of autobiographical memories. *J. Neurosci.* 23, 5302–5307.
- Maguire, E.A., Mullally, S.L., 2013. The hippocampus: a manifesto for change. *J. Exp. Psychol. Gen.* 142, 1180–1189. <https://doi.org/10.1037/a0033650>.
- Maguire, E.A., Mummery, C.J., 1999. Differential modulation of a common memory retrieval network revealed by positron emission tomography. *Hippocampus* 9, 54–61. [https://doi.org/10.1002/\(SICI\)1098-1063\(1999\)9:1<54::AID-HIPO6>3.0.CO;2-O](https://doi.org/10.1002/(SICI)1098-1063(1999)9:1<54::AID-HIPO6>3.0.CO;2-O).
- McCormick, C., Ciaramelli, E., De Luca, F., Maguire, E.A., 2017. Comparing and contrasting the cognitive effects of hippocampal and ventromedial prefrontal cortex damage: a review of human lesion studies. *Neuroscience*. <https://doi.org/10.1016/j.neuroscience.2017.07.066>.
- McCormick, C., St-Laurent, M., Ty, A., Valiante, T.A., McAndrews, M.P., 2015. Functional and effective hippocampal-neocortical connectivity during construction and elaboration of autobiographical memory retrieval. *Cerebr. Cortex* 25, 1297–1305. <https://doi.org/10.1093/cercor/bht324>.
- Moeller, S., Auerbach, E., Van de Moortele, P.F., Ugurbil, K., 2008. fMRI with 16 fold reduction using multiband multislice sampling. In: *Proceedings of the International Society for Magnetic Resonance in Medicine*.
- Nawa, N.E., Ando, H., 2018. Effects of vividness during the elaboration of autobiographical memories. In: *Presented at the Society for Neuroscience Annual Meeting*.
- Nieuwenhuis, I.L.C., Takashima, A., 2011. The role of the ventromedial prefrontal cortex in memory consolidation. *Behav. Brain Res.* 218, 325–334. <https://doi.org/10.1016/j.bbr.2010.12.009>.
- Oldfield, R.C., 1971. The assessment and analysis of handedness: the Edinburgh inventory. *Neuropsychologia* 9, 97–113. [https://doi.org/10.1016/0028-3932\(71\)90067-4](https://doi.org/10.1016/0028-3932(71)90067-4).
- Öngür, D., Ferry, A.T., Price, J.L., 2003. Architectonic subdivision of the human orbital and medial prefrontal cortex. *J. Comp. Neurol.* 460, 425–449. <https://doi.org/10.1002/cne.10609>.
- Öngür, D., Price, J.L., 2000. The organization of networks within the orbital and medial prefrontal cortex of rats, monkeys and humans. *Cerebr. Cortex* 10 (3), 206–219.
- Penny, W.D., Stephan, K.E., Daunizeau, J., Rosa, M.J., Friston, K.J., Schofield, T.M., Leff, A.P., 2010. Comparing families of dynamic causal models. *PLoS Comput. Biol.* 6 <https://doi.org/10.1371/journal.pcbi.1000709> e1000709–14.
- Phelps, E.A., 2004. Human emotion and memory: interactions of the amygdala and hippocampal complex. *Curr. Opin. Neurobiol.* 14, 198–202. <https://doi.org/10.1016/j.conb.2004.03.015>.
- Piefke, M., Weiss, P.H., Zilles, K., Markowitsch, H.J., Fink, G.R., 2003. Differential remoteness and emotional tone modulate the neural correlates of autobiographical memory. *Brain* 126, 650–668.
- Piolino, P., Desgranges, B., Eustache, F., 2009. Episodic autobiographical memories over the course of time: cognitive, neuropsychological and neuroimaging findings. *Neuropsychologia* 47, 2314–2329. <https://doi.org/10.1016/j.neuropsychologia.2009.01.020>.
- Poppenk, J., Evensmoen, H.R., Moscovitch, M., Nadel, L., 2013. Long-axis specialization of the human hippocampus. *Trends Cognit. Sci. (Regul. Ed.)* 17, 230–240. <https://doi.org/10.1016/j.tics.2013.03.005>.
- Preston, A.R., Eichenbaum, H., 2013. Interplay of Hippocampus and prefrontal review cortex in memory. *Curr. Biol.* 23, R764–R773. <https://doi.org/10.1016/j.cub.2013.05.041>.
- Raichle, M.E., 2015. The brain's default mode network. *Annu. Rev. Neurosci.* 38, 433–447. <https://doi.org/10.1146/annurev-neuro-071013-014030>.
- Raichle, M.E., MacLeod, A.M., Snyder, A.Z., Powers, W.J., Gusnard, D.A., Shulman, G.L., 2001. A default mode of brain function. *Proc. Natl. Acad. Sci. U.S.A.* 98, 676–682. <https://doi.org/10.1073/pnas.98.2.676>.
- Rissman, J., Chow, T.E., Reggente, N., Wagner, A.D., 2016. Decoding fMRI signatures of real-world autobiographical memory retrieval. *J. Cognit. Neurosci.* 28, 604–620. [https://doi.org/10.1162/jocn\\_a\\_00920](https://doi.org/10.1162/jocn_a_00920).
- Roy, M., Shohamy, D., Wager, T.D., 2012. Ventromedial prefrontal-subcortical systems and the generation of affective meaning. *Trends Cognit. Sci. (Regul. Ed.)* 16, 147–156. <https://doi.org/10.1016/j.tics.2012.01.005>.
- Rubin, R.D., Schwarb, H., Lucas, H., Dulias, M., Cohen, N., 2017. Dynamic hippocampal and prefrontal contributions to memory processes and representations blur the boundaries of traditional cognitive domains. *Brain Sci.* 7 <https://doi.org/10.3390/brainsci7070082>, 82–17.
- Rubin, R.D., Watson, P.D., Duff, M.C., Cohen, N.J., 2014. The role of the hippocampus in flexible cognition and social behavior. *Front. Hum. Neurosci.* 8, 742. <https://doi.org/10.3389/fnhum.2014.00742>.
- Ryan, L., Nadel, L., Keil, K., Putnam, K., Schnyer, D., Trouard, T., Moscovitch, M., 2001. Hippocampal complex and retrieval of recent and very remote autobiographical memories: evidence from functional magnetic resonance imaging in neurologically intact people. *Hippocampus* 11, 707–714. <https://doi.org/10.1002/hipo.1086>.
- Saunders, R.C., Rosene, D.L., Van Hoesen, G.W., 1988. Comparison of the efferents of the amygdala and the hippocampal formation in the rhesus monkey: II. Reciprocal and non-reciprocal connections. *J. Comp. Neurol.* 271, 185–207. <https://doi.org/10.1002/cne.902710203>.
- Schacter, D.L., Addis, D.R., Buckner, R.L., 2007. Remembering the Past to Imagine the Future: the Prospective Brain, vol. 8. Nature Publishing Group, pp. 657–661. <https://doi.org/10.1038/nrn2213>.
- Schacter, D.L., Addis, D.R., Hassabis, D., Martin, V.C., Spreng, R.N., Szpunar, K.K., 2012. The future of memory: remembering, imagining, and the brain. *Neuron* 76, 677–694. <https://doi.org/10.1016/j.neuron.2012.11.001>.
- Schacter, D.L., Norman, K.A., Koutstaal, W., 1998. The cognitive neuroscience of constructive memory. *Annu. Rev. Psychol.* 49, 289–318. <https://doi.org/10.1146/annurev.psych.49.1.289>.
- Schneider, B., Koenigs, M., 2017. Human lesion studies of ventromedial prefrontal cortex. *Neuropsychologia* 107, 84–93. <https://doi.org/10.1016/j.neuropsychologia.2017.09.035>.
- Seghier, M.L., Josse, G., Leff, A.P., Price, C.J., 2010. Lateralization is predicted by reduced coupling from the left to right prefrontal cortex during semantic decisions on written words. *Cerebr. Cortex* 21, 1519–1531. <https://doi.org/10.1093/cercor/bhq203>.
- Seidnitz, L., Diener, E., 1998. Sex differences in the recall of affective experiences. *J. Pers. Soc. Psychol.* 74, 262–271.
- Sharot, T., Riccardi, A.M., Raio, C.M., Phelps, E.A., 2007. Neural mechanisms mediating optimism bias. *Nature* 450, 102–105. <https://doi.org/10.1038/nature06280>.
- Simons, J.S., Spiers, H.J., 2003. Prefrontal and medial temporal lobe interactions in long-term memory. *Nat. Rev. Neurosci.* 4, 637–648. <https://doi.org/10.1038/nrn1178>.
- Smith, S.M., Miller, K.L., Salimi-Khorshidi, G., Webster, M., Beckmann, C.F., Nichols, T.E., Ramsey, J.D., Woolrich, M.W., 2011. Network modelling methods for FMRI. *Neuroimage* 54, 875–891. <https://doi.org/10.1016/j.neuroimage.2010.08.063>.
- Spalding, K.N., Jones, S.H., Duff, M.C., Tranel, D., Warren, D.E., 2015. Investigating the neural correlates of schemas: ventromedial prefrontal cortex is necessary for normal schematic influence on memory. *J. Neurosci.* 35, 15746–15751. <https://doi.org/10.1523/JNEUROSCI.2767-15.2015>.
- Speer, M.E., Bhanji, J.P., Delgado, M.R., 2014. Savoring the past: positive memories evoke value representations in the striatum. *Neuron* 84, 847–856. <https://doi.org/10.1016/j.neuron.2014.09.028>.
- Spreng, R.N., Grady, C.L., 2010. Patterns of brain activity supporting autobiographical memory, prospection, and theory of mind, and their relationship to the default mode network. *J. Cognit. Neurosci.* 22, 1112–1123. <https://doi.org/10.1162/jocn.2009.21282>.
- Spreng, R.N., Mar, R.A., Kim, A.S.N., 2009. The common neural basis of autobiographical memory, prospection, navigation, theory of mind, and the default mode: a quantitative meta-analysis. *J. Cognit. Neurosci.* 21, 489–510. <https://doi.org/10.1162/jocn.2008.21029>.
- Stephan, K.E., Penny, W.D., Moran, R.J., Oudén, H.E.M., Daunizeau, J., Friston, K.J., 2010. Ten simple rules for dynamic causal modeling. *Neuroimage* 49, 3099–3109. <https://doi.org/10.1016/j.neuroimage.2009.11.015>.
- Suddendorf, T., Addis, D.R., Corballis, M.C., 2009. Mental time travel and the shaping of the human mind. *Philos. Trans. R. Soc. Lond. B Biol. Sci.* 364, 1317–1324. <https://doi.org/10.1098/rstb.2008.0301>.
- Svoboda, E., McKinnon, M.C., Levine, B., 2006. The functional neuroanatomy of autobiographical memory: a meta-analysis. *Neuropsychologia* 44, 2189–2208. <https://doi.org/10.1016/j.neuropsychologia.2006.05.023>.
- Talarico, J.M., LaBar, K.S., Rubin, D.C., 2004. Emotional intensity predicts autobiographical memory experience. *Mem. Cognit.* 32, 1118–1132.
- Tulving, E., 1985. Memory and consciousness. *Can. Psychol.* 26, 1–12.
- van Kesteren, M.T.R., Ruiter, D.J., Fernández, G., Henson, R.N.A., 2012. How schema and novelty augment memory formation. *Trends Neurosci.* 35, 211–219. <https://doi.org/10.1016/j.tins.2012.02.001>.
- Viard, A., Piolino, P., Desgranges, B., Chetelat, G., Lebreton, K., Landeau, B., Young, A., La Sayette, D., Eustache, F., 2007. Hippocampal activation for autobiographical memories over the entire lifetime in healthy aged subjects: an fMRI study. *Cerebr. Cortex* 17, 2453–2467. <https://doi.org/10.1093/cercor/bhl153>.
- Watson, D., Clark, L.A., Tellegen, A., 1988. Development and validation of brief measures of positive and negative affect: the PANAS scales. *J. Pers. Soc. Psychol.* 54, 1063–1070. <https://doi.org/10.1037/0022-3514.54.6.1063>.
- Wheeler, M.A., Stuss, D.T., Tulving, E., 1997. Toward a theory of episodic memory: the frontal lobes and autonoetic consciousness. *Psychol. Bull.* 121, 331–354.
- Wincoff, A., Clithero, J.A., Carter, R.M., Bergman, S.R., Wang, L., Huettel, S.A., 2013. Ventromedial prefrontal cortex encodes emotional value. *J. Neurosci.* 33, 11032–11039. <https://doi.org/10.1523/JNEUROSCI.4317-12.2013>.
- Young, K.D., Siegle, G.J., Bodurka, J., Drevets, W.C., 2016. Amygdala activity during autobiographical memory recall in depressed and vulnerable individuals: association with symptom severity and autobiographical overgenerality. *Am. J. Psychiatry* 173, 78–89. <https://doi.org/10.1176/appi.ajp.2015.15010119>.
- Yushkevich, P.A., Pluta, J.B., Wang, H., Xie, L., Ding, S.-L., Gertje, E.C., Mancuso, L., Klödt, D., Das, S.R., Wolk, D.A., 2014. Automated volumetry and regional thickness analysis of hippocampal subfields and medial temporal cortical structures in mild cognitive impairment. *Hum. Brain Mapp.* 36, 258–287. <https://doi.org/10.1002/hbm.22627>.
- Zald, D.H., Andreotti, C., 2010. Neuropsychological assessment of the orbital and ventromedial prefrontal cortex. *Neuropsychologia* 48, 3377–3391. <https://doi.org/10.1016/j.neuropsychologia.2010.08.012>.
- Zeidman, P., Maguire, E.A., 2016. Anterior hippocampus: the anatomy of perception, imagination and episodic memory. *Nat. Rev. Neurosci.* 17, 173–182. <https://doi.org/10.1038/nrn.2015.24>.